

When scale-separation helps: three examples in MHD

Annick Pouquet

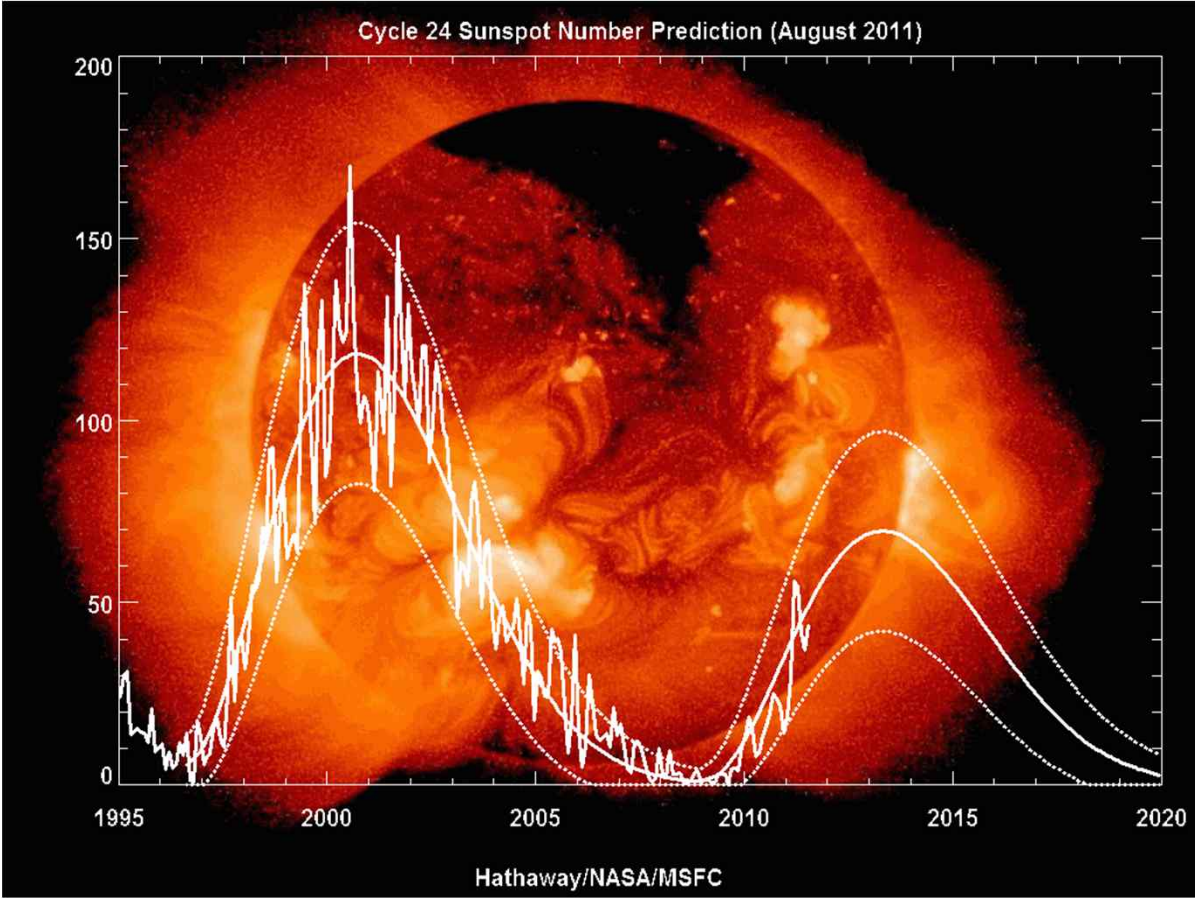
*Erik Blackman (Rochester), Marc-Etienne Brachet (ENS, Paris),
Jonathan Pietarila-Graham (LANL), Pablo Mininni[^],
and Duane Rosenberg*

[^]also at Universidad de Buenos Aires

Pohang, November 2011

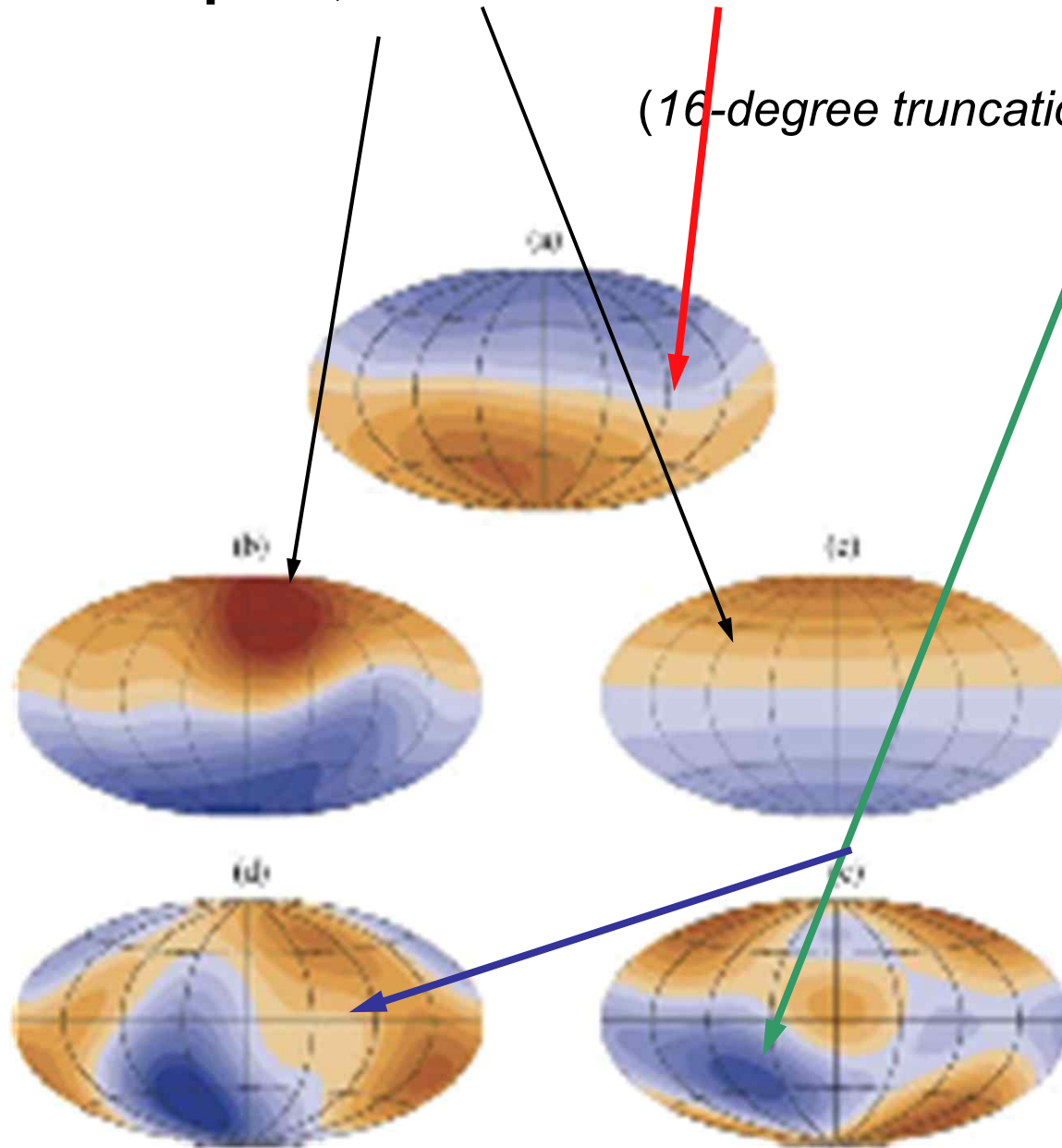
pouquet@ucar.edu





Surface (1 bar) radial magnetic fields for Jupiter, Saturne & Earth versus Uranus & Neptune

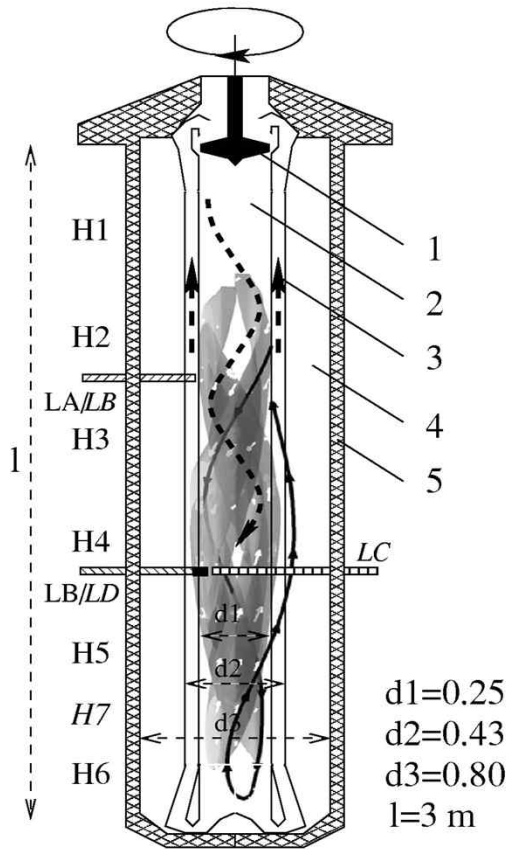
(16-degree truncation, Sabine Stanley, 2006)



Axially dipolar

Quadrupole ~ dipole

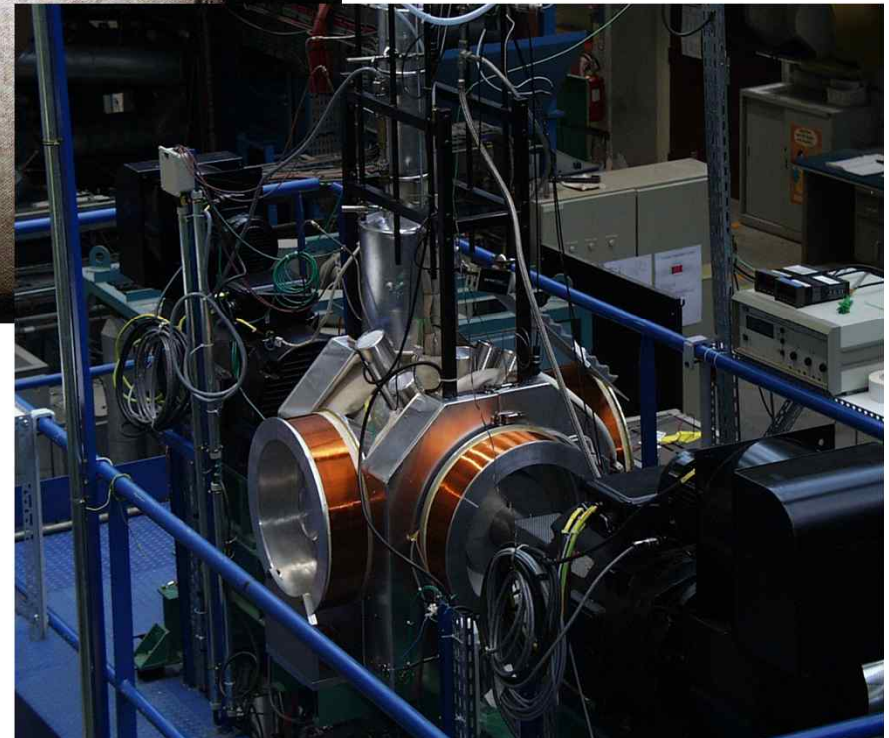
Dynamo Experiments



Riga



Karlsruhe



Cadarache

The MHD equations

Multi-scale interactions (high Reynolds), to the detriment of all other concerns

- P is the pressure, $\mathbf{j} = \nabla \times \mathbf{B}$ is the current, \mathbf{F} is an external force, ν is the viscosity, η the resistivity, \mathbf{v} the velocity and \mathbf{B} the induction (in Alfvén velocity units); **incompressibility** is assumed, and $\text{div}.\mathbf{B} = 0$.

$$\frac{\partial \mathbf{v}}{\partial t} + \mathbf{v} \cdot \nabla \mathbf{v} = -\nabla P + \mathbf{j} \times \mathbf{B} + \nu \nabla^2 \mathbf{v} + \mathbf{F}$$
$$\frac{\partial \mathbf{B}}{\partial t} + \mathbf{v} \cdot \nabla \mathbf{B} = \mathbf{B} \cdot \nabla \mathbf{v} + \eta \nabla^2 \mathbf{B} ,$$

The MHD equations

Multi-scale interactions (high Reynolds), to the detriment of all other concerns

- P is the pressure, $\mathbf{j} = \nabla \times \mathbf{B}$ is the current, \mathbf{F} is an external force, ν is the viscosity, η the resistivity, \mathbf{v} the velocity and \mathbf{B} the induction (in Alfvén velocity units); **incompressibility** is assumed, and $\text{div.}\mathbf{B} = 0$.

$$\frac{\partial \mathbf{v}}{\partial t} + \mathbf{v} \cdot \nabla \mathbf{v} = -\nabla P + \mathbf{j} \times \mathbf{B} + \nu \nabla^2 \mathbf{v} + \mathbf{F}$$
$$\frac{\partial \mathbf{B}}{\partial t} + \mathbf{v} \cdot \nabla \mathbf{B} = \mathbf{B} \cdot \nabla \mathbf{v} + \eta \nabla^2 \mathbf{B} ,$$

Ideal case: $\nu=0$ and $\eta=0 \rightarrow 3$ quadratic invariants

Parameters in MHD

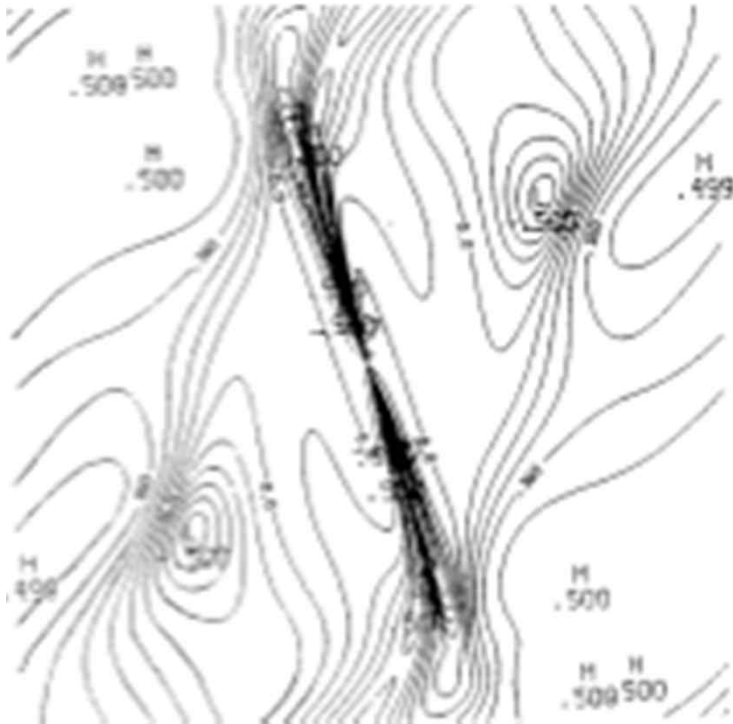
- $R_V = U_{\text{rms}} L_0 / \nu \gg 1$
- Magnetic Reynolds number $R_M = U_{\text{rms}} L_0 / \eta$
Magnetic Prandtl number: $P_M = R_M / R_V = \nu / \eta$
 P_M is high in the interstellar medium.
 P_M is low in the solar convection zone, in the liquid core of the Earth, in liquid metals and in laboratory experiments
And $P_M \sim 1$ in most numerical experiments until recently ...
- Energy ratio E_M/E_V or time-scale ratio T_{NL}/T_A
with $T_{NL} = l/u_l$ and $T_A = l/b$
- (Quasi-) Uniform magnetic field \mathbf{B}_0
- Magnetic & cross helicity $H^M = \langle \mathbf{A} \cdot \mathbf{B} \rangle$ & $H_c = \langle \mathbf{v} \cdot \mathbf{B} \rangle$ (invariants, as $E_M + E_V$)
- *Boundaries, geometry, rotation, stratification, cosmic rays, radiation, ...*

Three examples for which scale separation helps

- Dynamics of two- & three-dimensional structures
- Dissipative turbulent behavior of a flow in the ideal non-dissipative case in two and three dimensions
- Does scale-separation for scales larger than the forcing scale help in the large-scale helical dynamo problem, at fixed Reynolds number?

Numerical set-up for Case 1

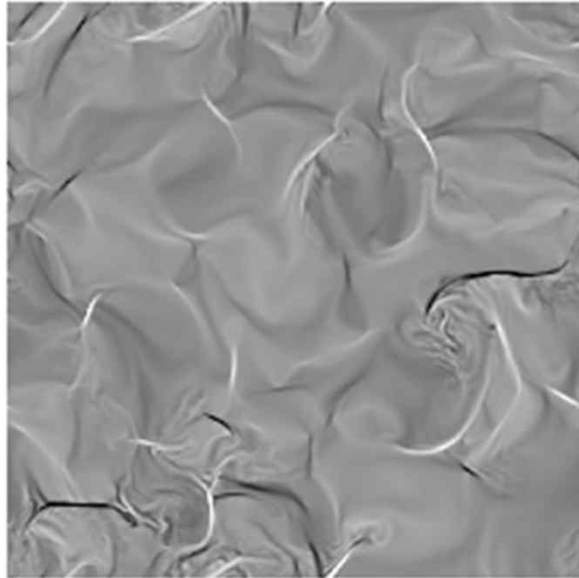
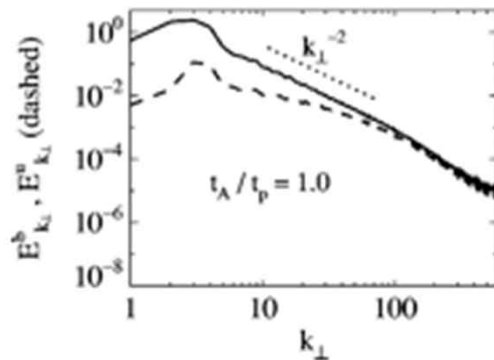
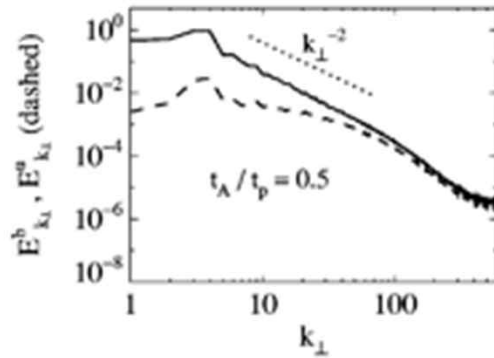
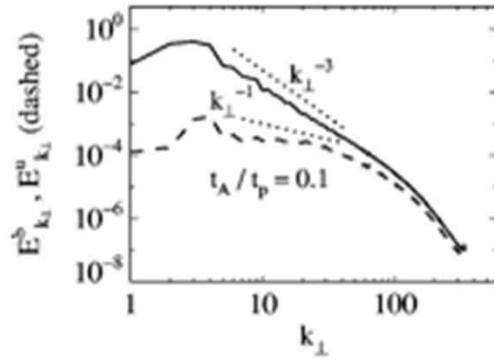
- Pseudo-spectral codes, 2D or 3D, MHD or RMHD, up to resolutions of 1536^3 grid points, some runs with imposed B_0 , initial conditions centered at large scale, mostly periodic b.c.
- 2D: Orszag-Tang (OT) vortex of a central X-point at a stagnation point
- 3D: Extension of the OT vortex, or random initial conditions



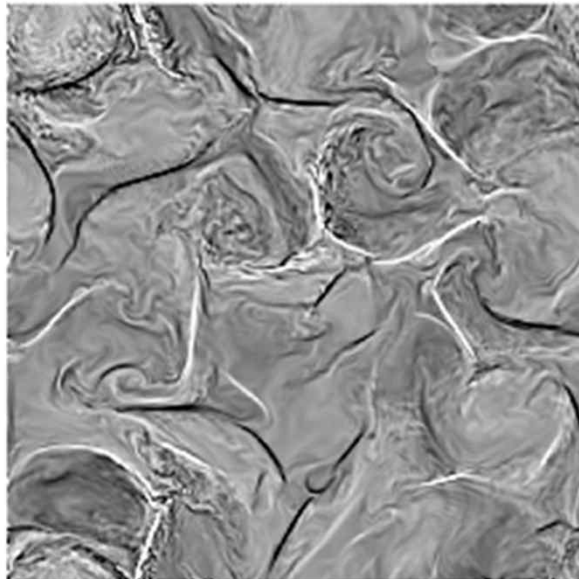
2D-MHD- Contours of $r_2(\mathbf{x}) = \mathbf{v} \cdot \mathbf{B} / [v^2 + b^2]$: local plages of maximal correlations ($r_2 = 0.5$) except in the central current sheet of the Orszag-Tang vortex -- for which globally, $r_2 = 0.25$
 (Meneguzzi et al., JCP 123, 32 (1996))

Contours of $\cos(\mathbf{v}, \mathbf{B})$, weak global correlation of 10^{-4}
 (Matthaeus et al., PRL 2008)





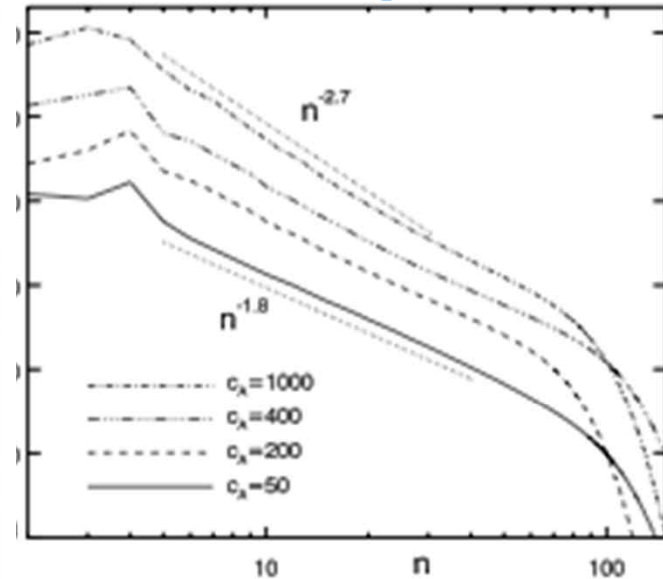
$t_A/t_p = 0.5$



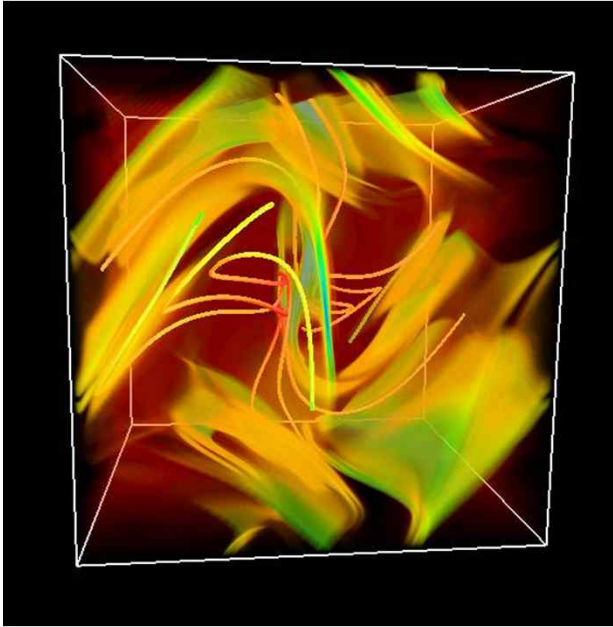
Reduced MHD Numerical data

Different T_A/T_{driver}

Rapazzo et al., 2008



8.—: Total energy spectra as a function of the wavenumber n for simulations F, G, H and I. To higher values of $c_A = v_A/u_{ph}$, the ratio between the Alfvén and photospheric velocities, correspond steeper spectra, with a power-law index respectively 1.8, 2, 2.3 and 2.7.

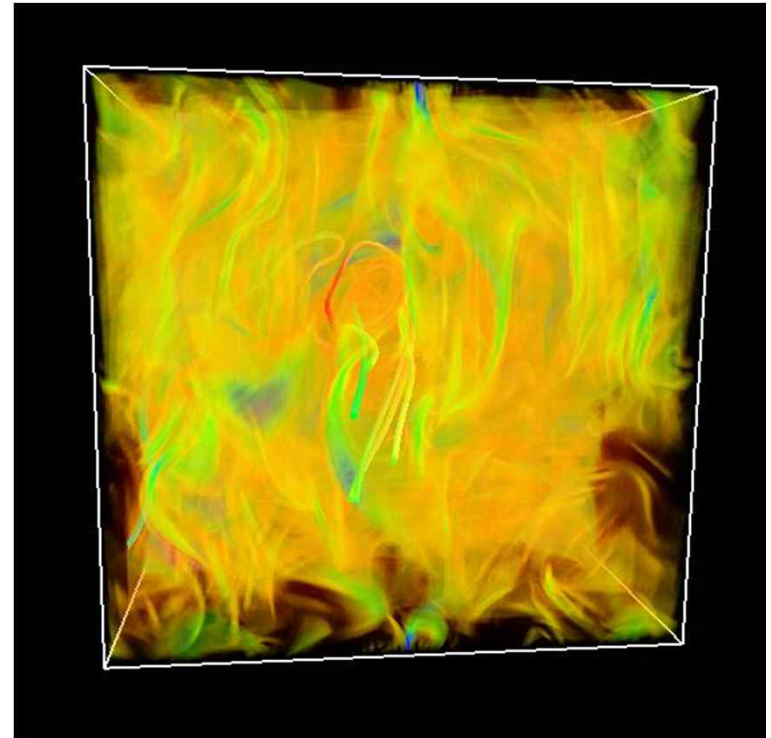


Current sheets for
3D-X point initial
configuration

512³ grid

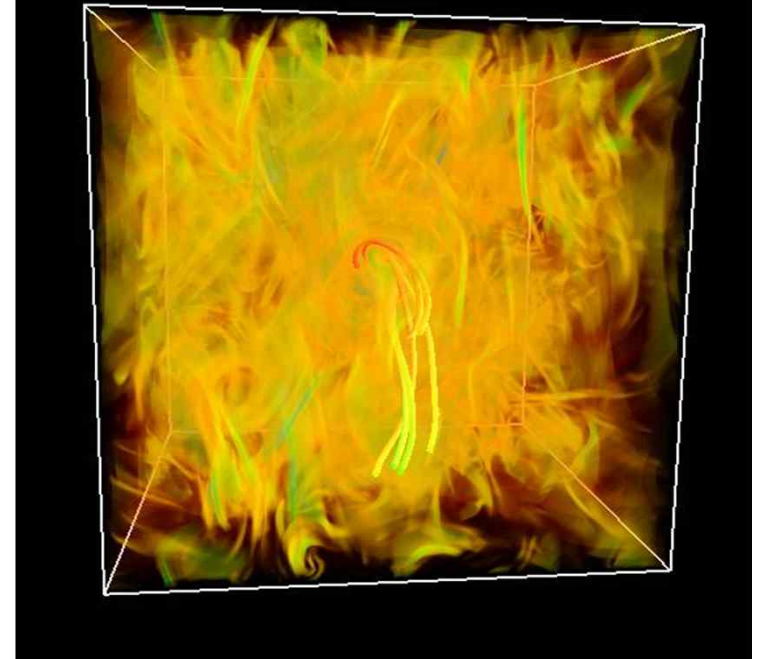
<-- t=0.5

t=0.9 -->



t=1.2 -->

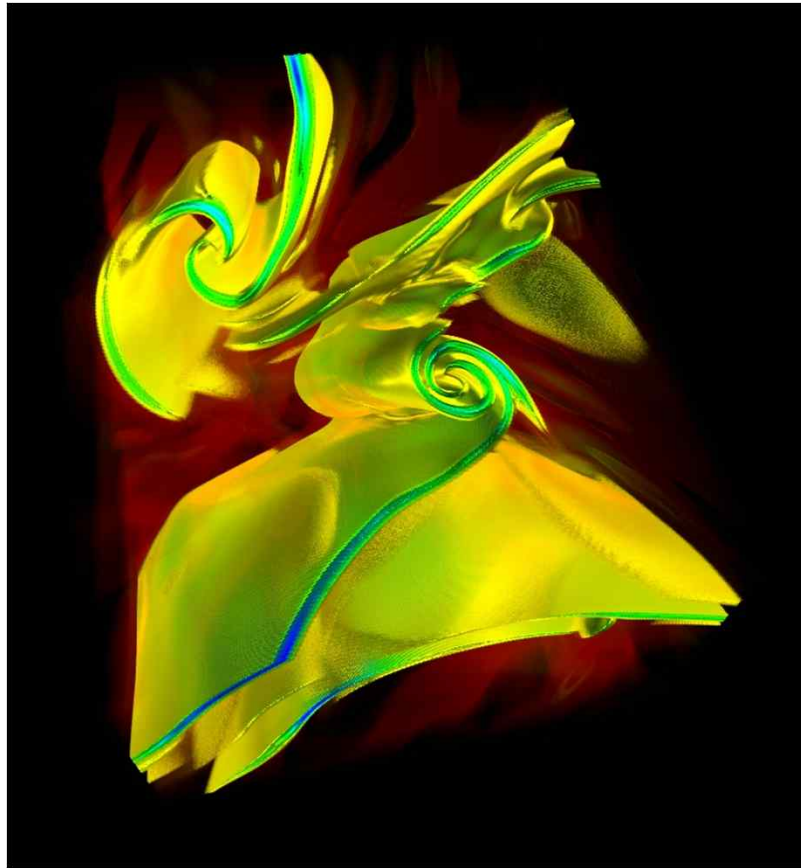
*Large-scale
order/memory?*



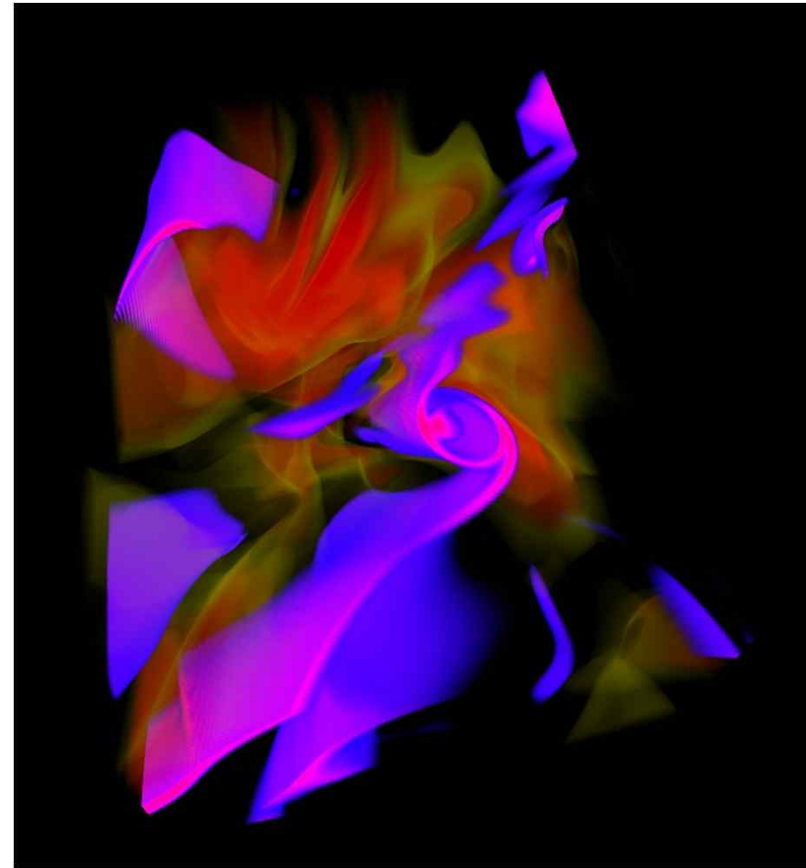
V and **B** are aligned in rolled-up current sheet,
but not equal ($B^2 \sim 2V^2$)

(Alexandrova et al., JGR 2006; Petviashvili & Pokhotolov, 1992)

1536³
decay
3D MHD
run



Early time (end of ideal phase)



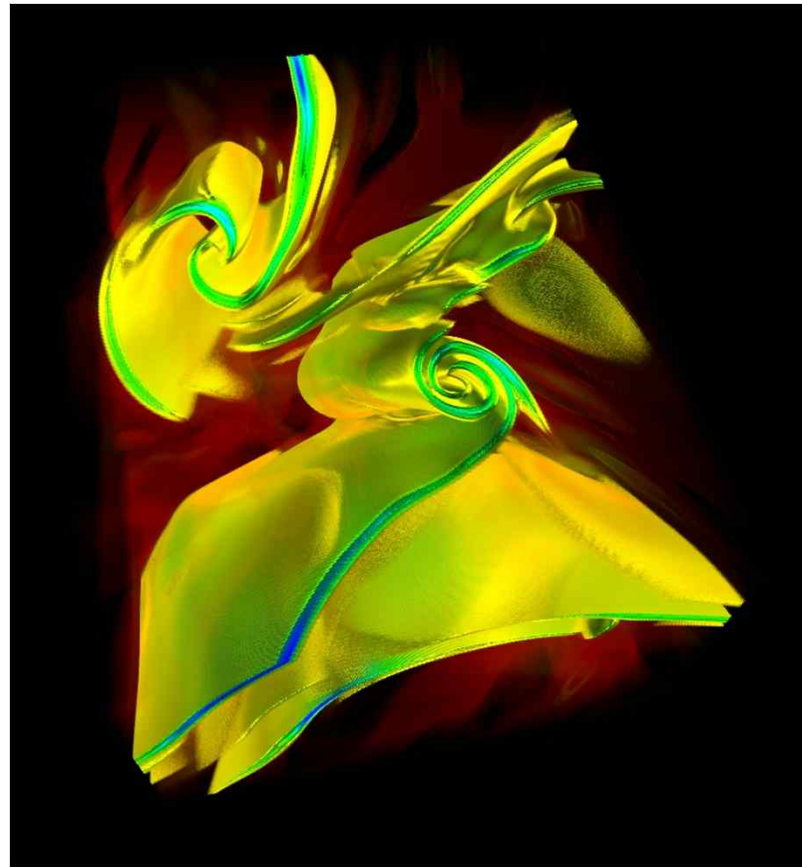
J^2

$\cos(\mathbf{V}, \mathbf{B})$

VAPOR freeware, cisl.ucar.edu/hss/dasg/software/vapor

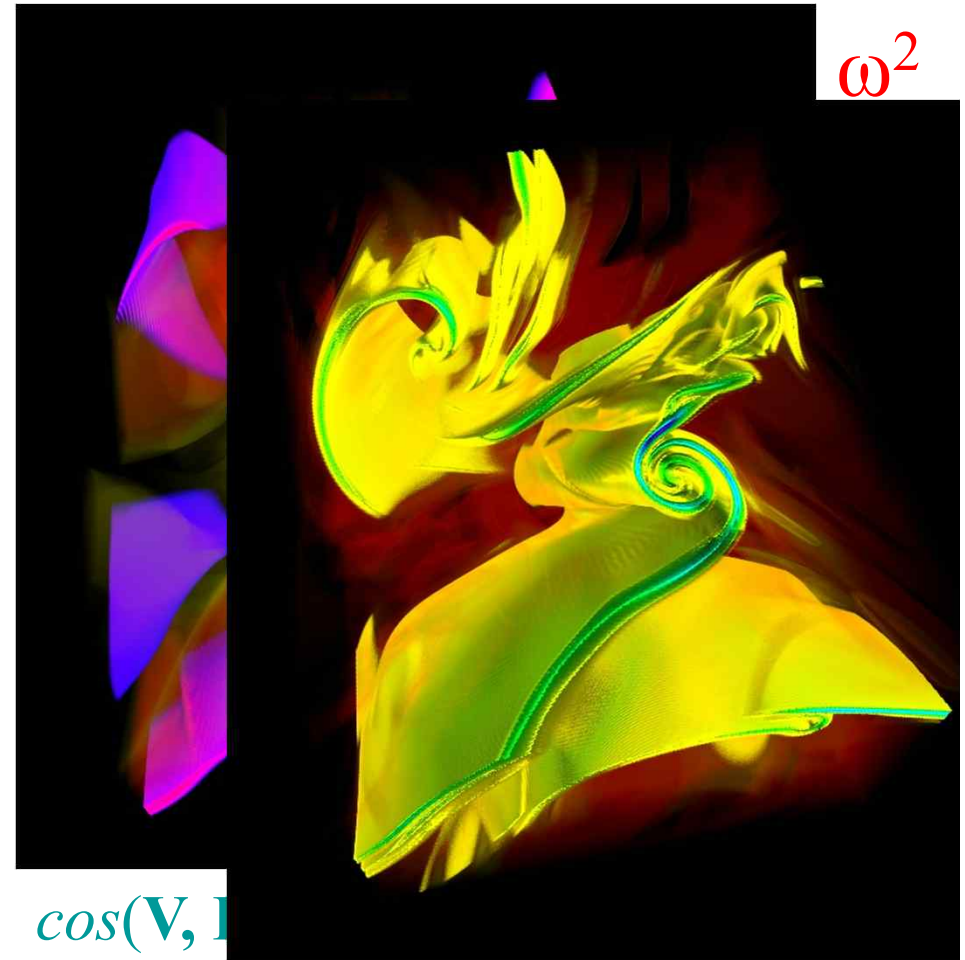
V and **B** are aligned in rolled-up current sheet, **so**
are J and ω

(Petviashvili & Pokhotolov, 1992. Solar Wind: Alexandrova et al., JGR 2006)



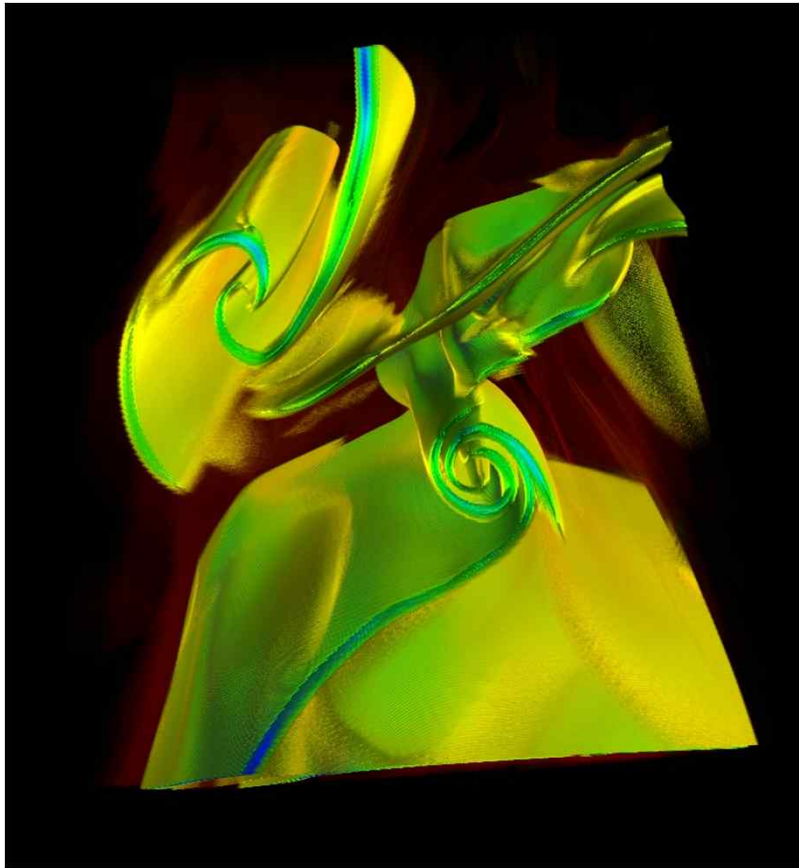
J^2

Early time (end of ideal phase)



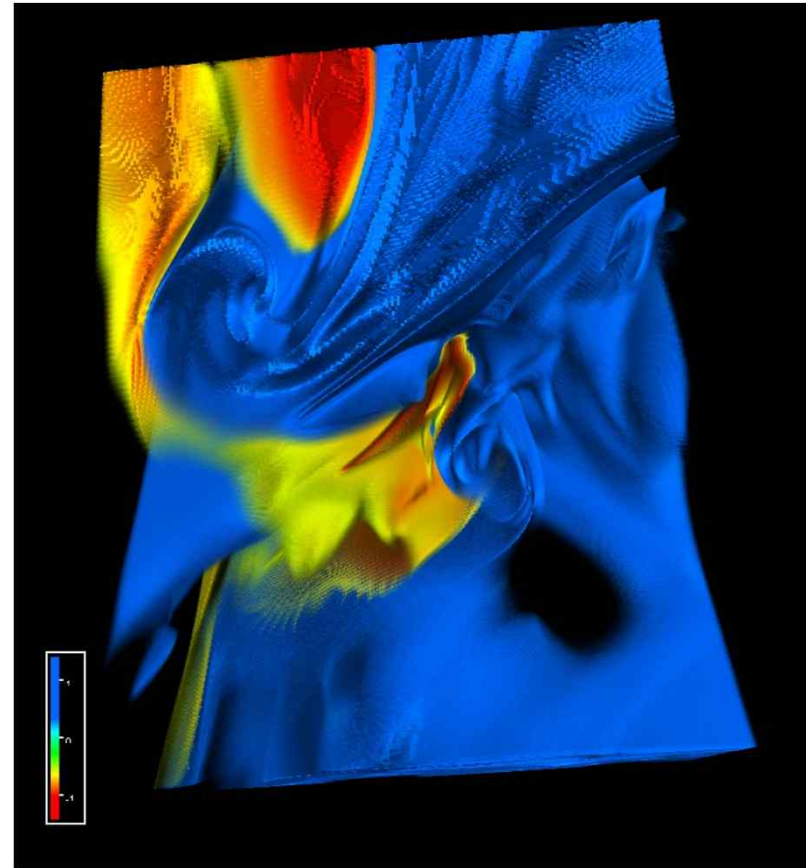
$\cos(\mathbf{V}, \mathbf{B})$

Strong *relative magnetic helicity* (~ 1):
change of topology across sheet



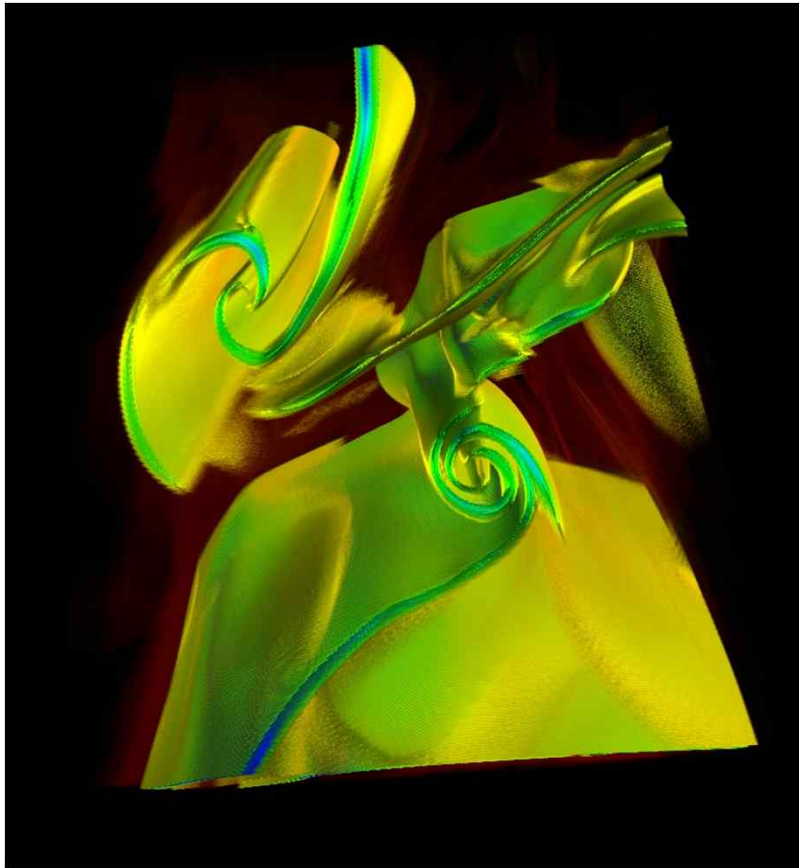
Current J^2

1536³ run, early time



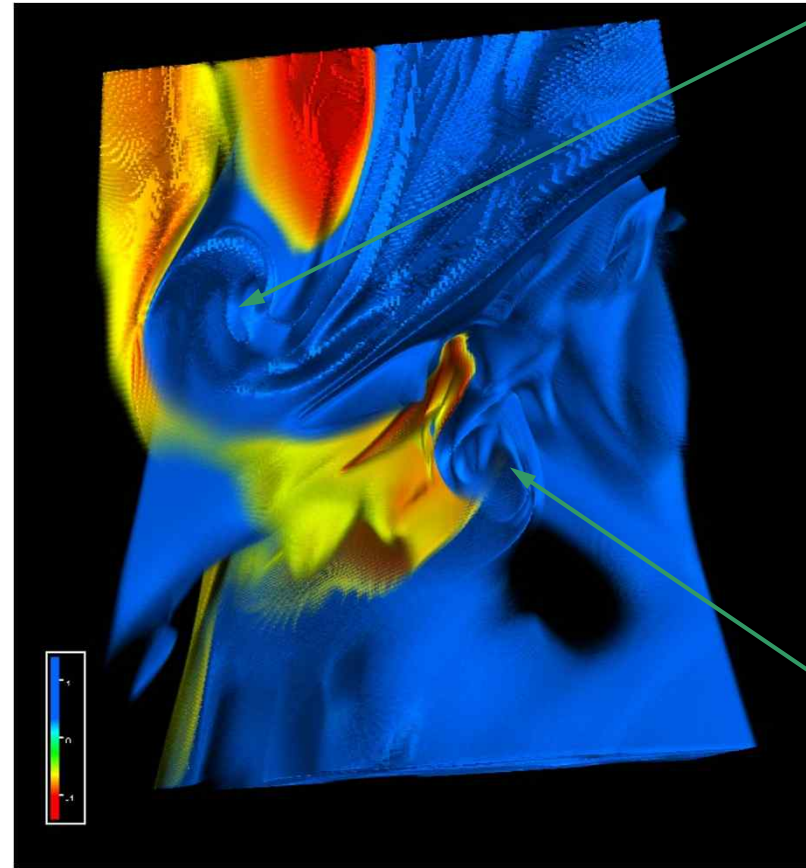
$\cos(\mathbf{A}, \mathbf{B})$, with $\mathbf{B} = \text{curl } \mathbf{A}$

Strong *relative magnetic helicity* (~ 1):
change of topology across sheet



Current J^2

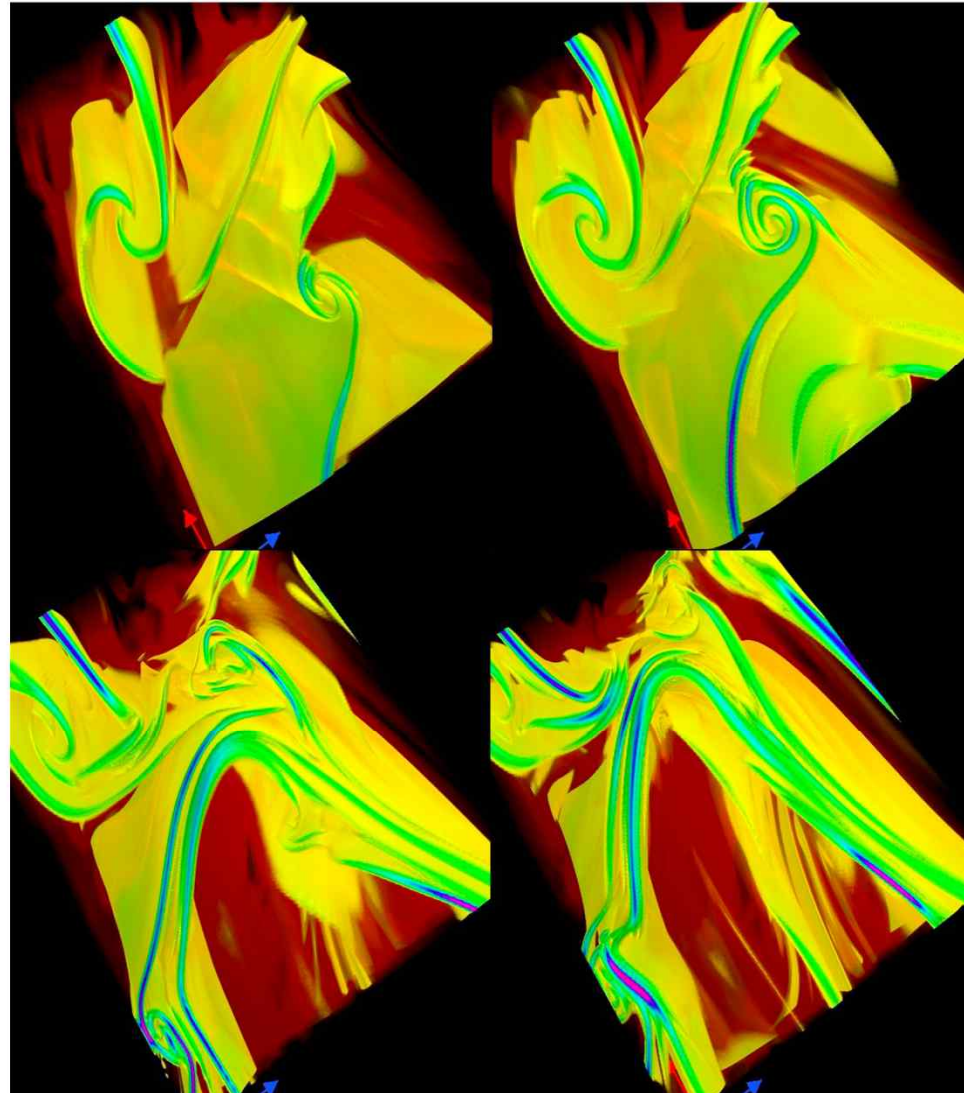
1536³ run, early time



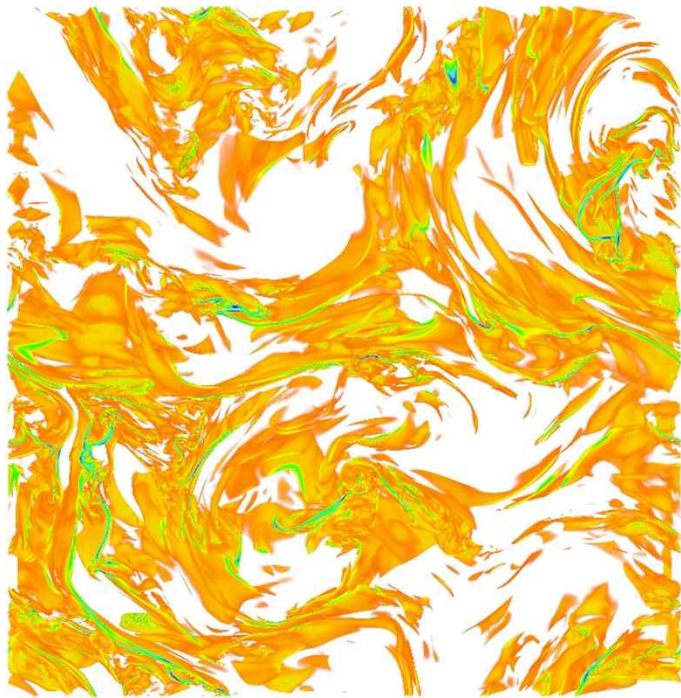
$\cos(\mathbf{A}, \mathbf{B})$, with $\mathbf{B} = \text{curl } \mathbf{A}$

Zoom on a current roll-up/sheet evolution

1536³ run

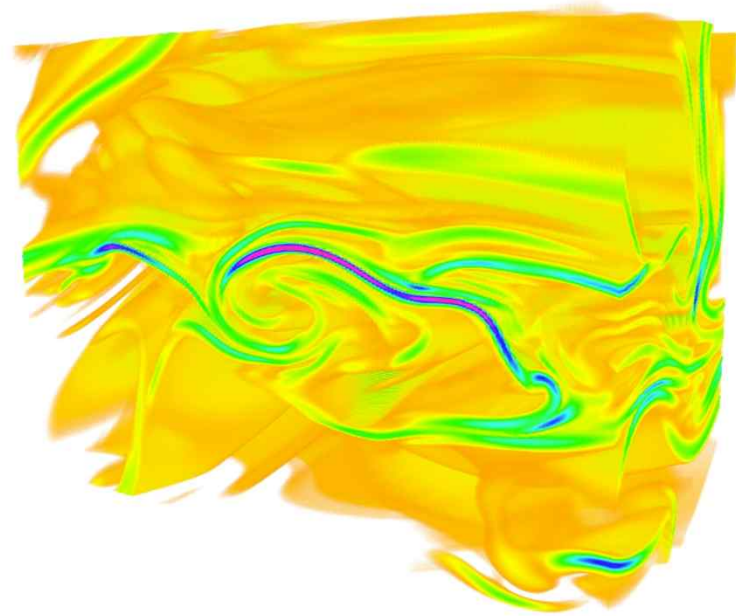


Current at peak of dissipation:
Both piling-up of sheets and folding



Global view
1536³ run

Zoom



Extreme events in direct numerical simulations of incompressible MHD

- Scaling exponents, 512^3 DNS with varying B_0 :
as B_0 increases, so does the intermittency

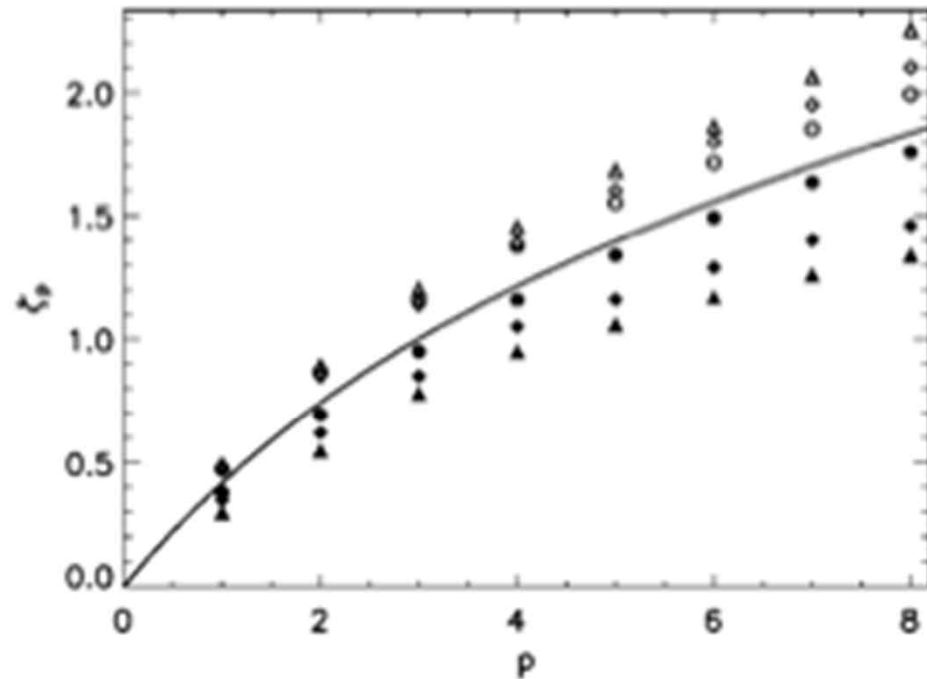


FIG. 1. Scaling exponents ζ_p of perpendicular (filled symbols) and parallel (open symbols) structure functions $S_p(\ell) = \langle |\delta z_\ell|^p \rangle$ for $B_0 = 0.5, 10$ (circles, diamonds, triangles) together with isotropic

Extreme events in solar active regions

- Scaling exponents of structure functions of magnetic field (magnetograms): more intermittency (more curvature) for more energetic flares

Abramenko, review (2007)

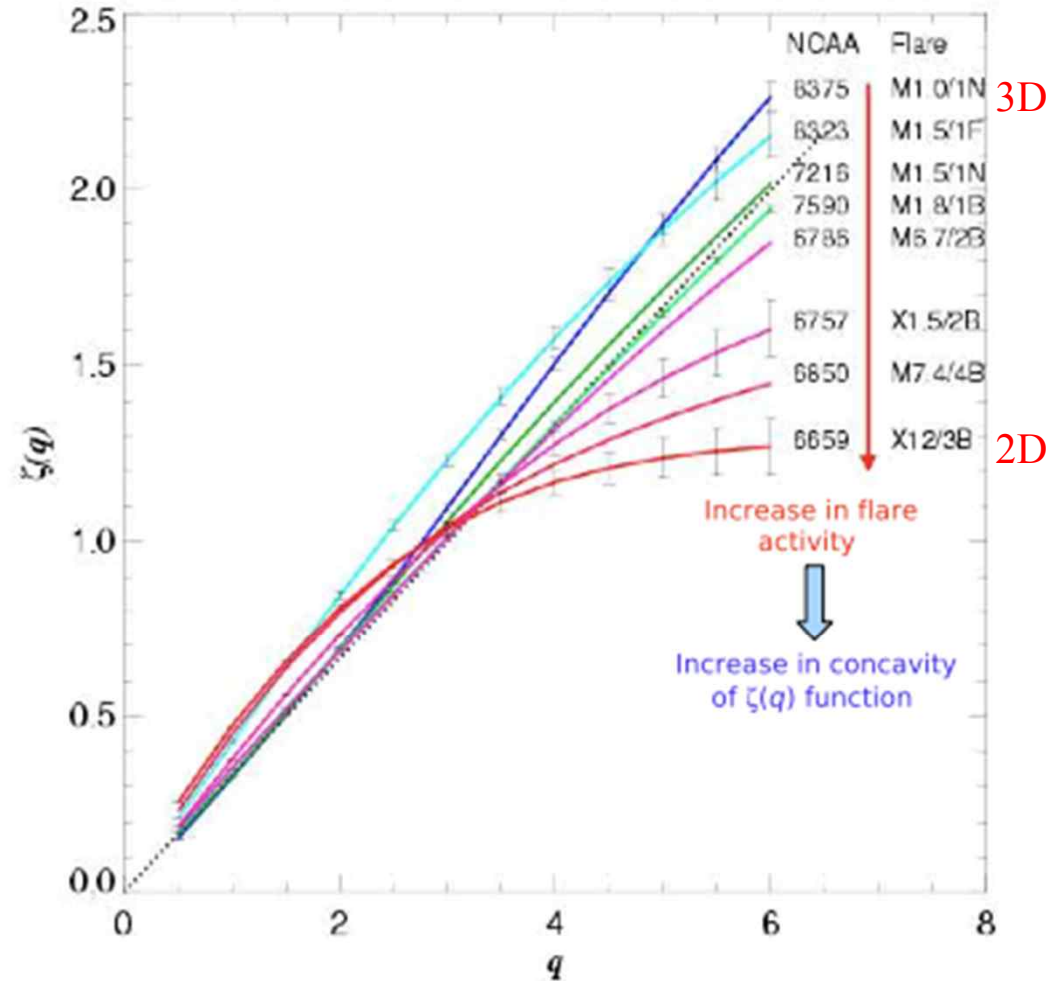
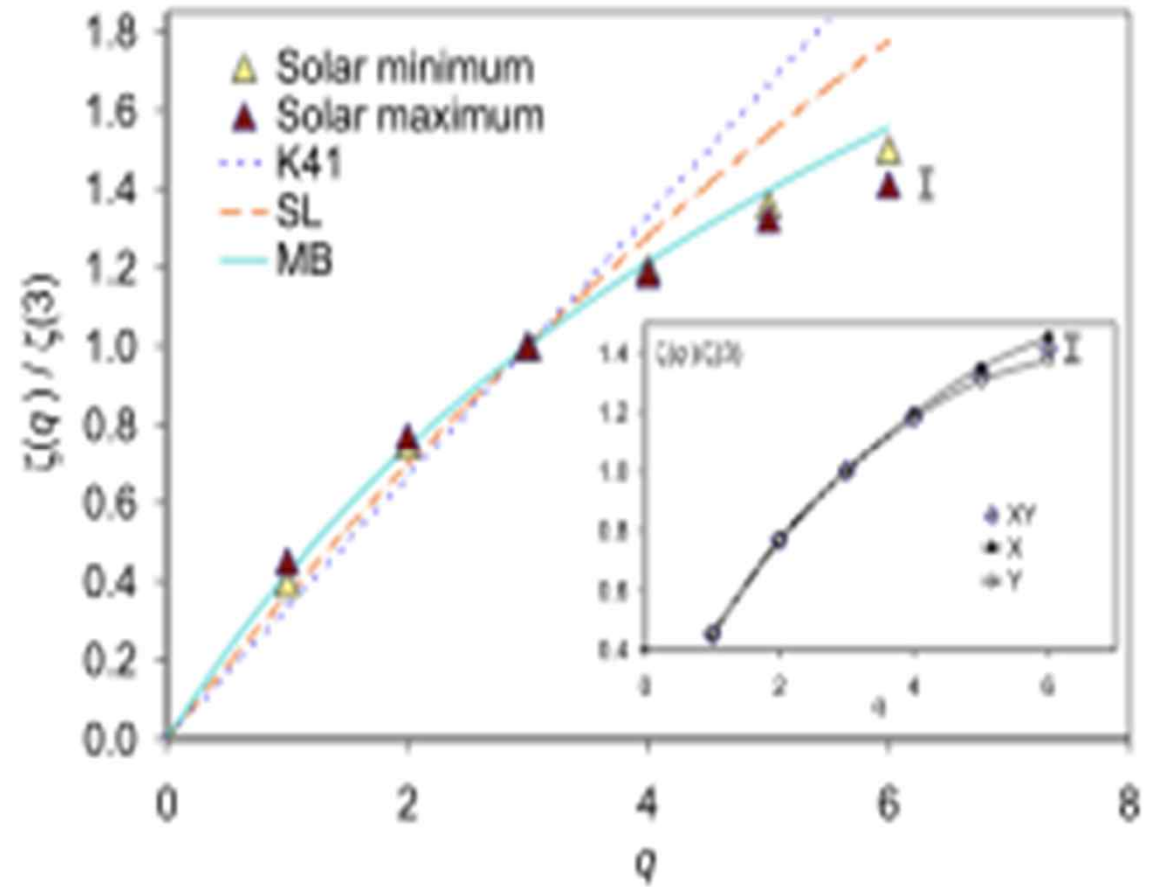


Figure 16: Scaling exponents $\zeta(q)$ of structure functions of order q calculated for eight active regions by Abramenko et al. (2002). The straight dotted line has a slope of $1/3$ and refers to the state of Kolmogorov turbulence. The NOAA number and the strongest flare (X-ray class/optical class) of each active region is shown. Increase of the flaring activity of active regions (from the top down to the bottom) is accompanied by general increase in concavity of $\zeta(q)$ functions.

- Solar corona extreme events (SOHO EIT 195A)
7000+ images (central part of full-disk)



Second case study:

**Ideal (non-dissipative) dynamics
of 2D and 3D MHD flows**

Numerical set-up for Case 2

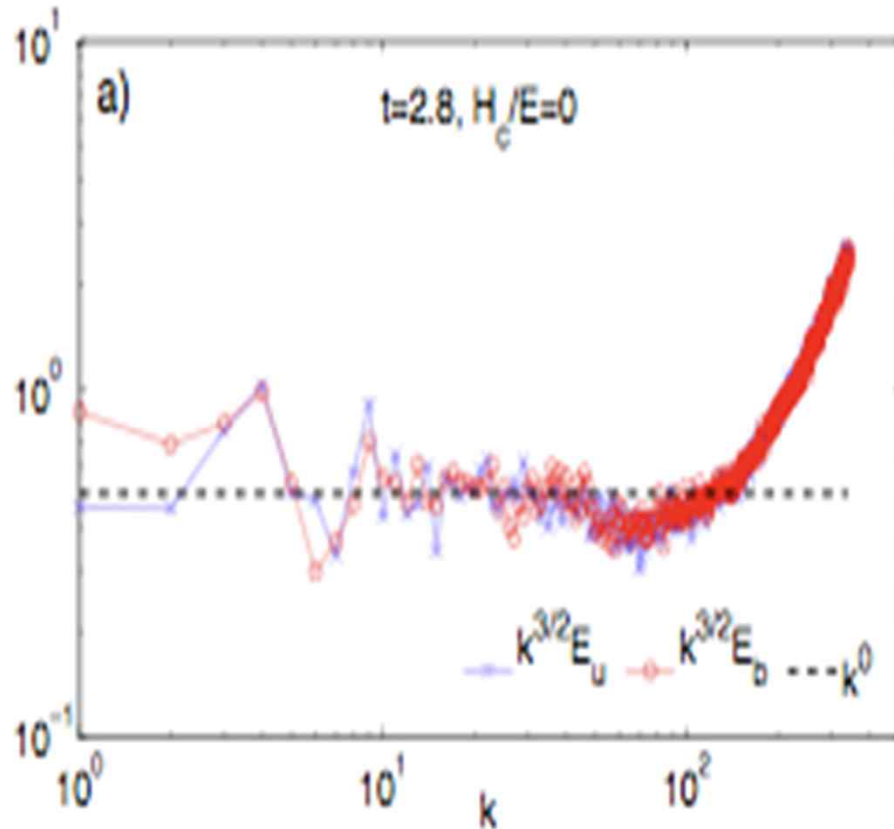
- **Ideal dynamics**, pseudo-spectral code, de-aliasing using the 2/3 rule & periodic boundary conditions, with **imposed 4-fold symmetries** in 3D
- No imposed B_0 , no forcing, no dissipation
- Up to 4096^2 grid points in 2D, and up to an *equivalent* resolution of 6144^3 in 3D
- 2D: Orszag-Tang vortex (OT)
- 3D: the velocity is the Taylor-Green (TG) flow, and the magnetic field has the same symmetries as TG; both are at the largest resolved scale initially

What to expect

- Long-time properties of truncated system of Fourier modes obey statistical mechanics compatible with all quadratic invariants → possibility of inverse cascades, lack of equipartition due to non-zero magnetic helicity, ...
- Small-scales thermalize faster than large-scales: the small-scale spectra provide a turbulent “dissipativity” in a 2-fluid model (large-scale vs. small-scale)
- What is the result?

Ideal MHD in two dimensions ($\nu=0$ and $\eta=0$):

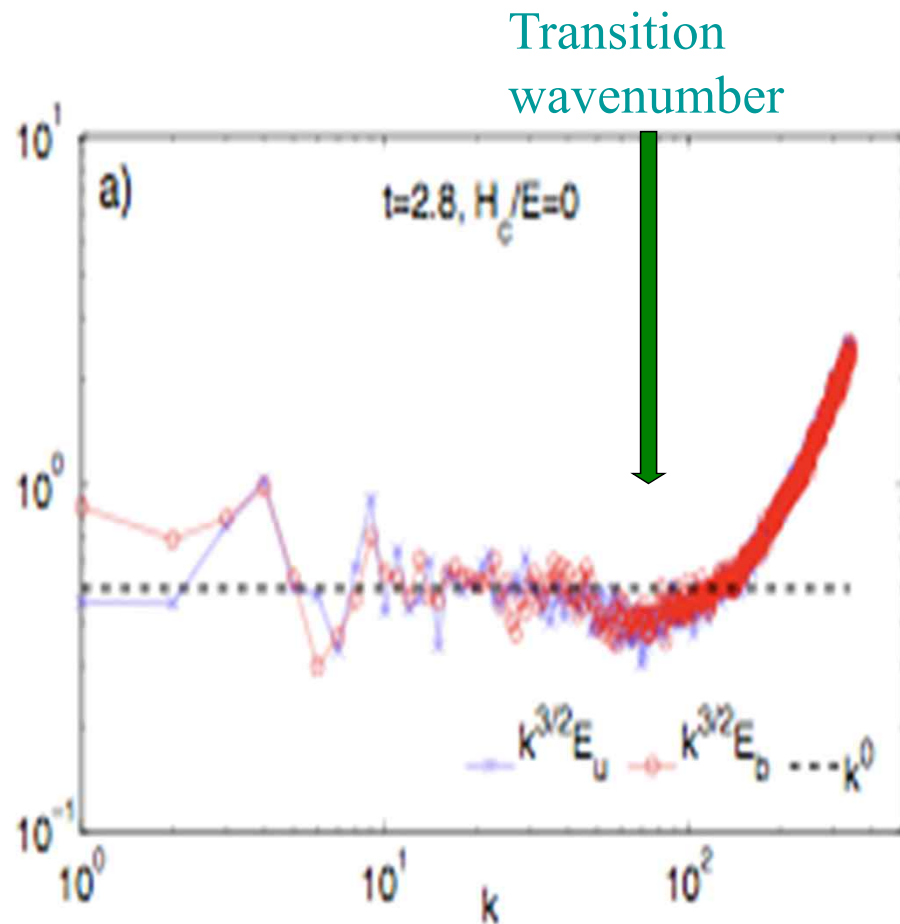
Kinetic & magnetic energy spectra, compensated by $k^{3/2}$



Intermediate temporal phase:
the small-scale thermalized k^{D-1}
spectra act as eddy diffusivities
for the “turbulent” dynamics at
intermediate scales

3D Euler: Cichowlas et al., PRL 2005

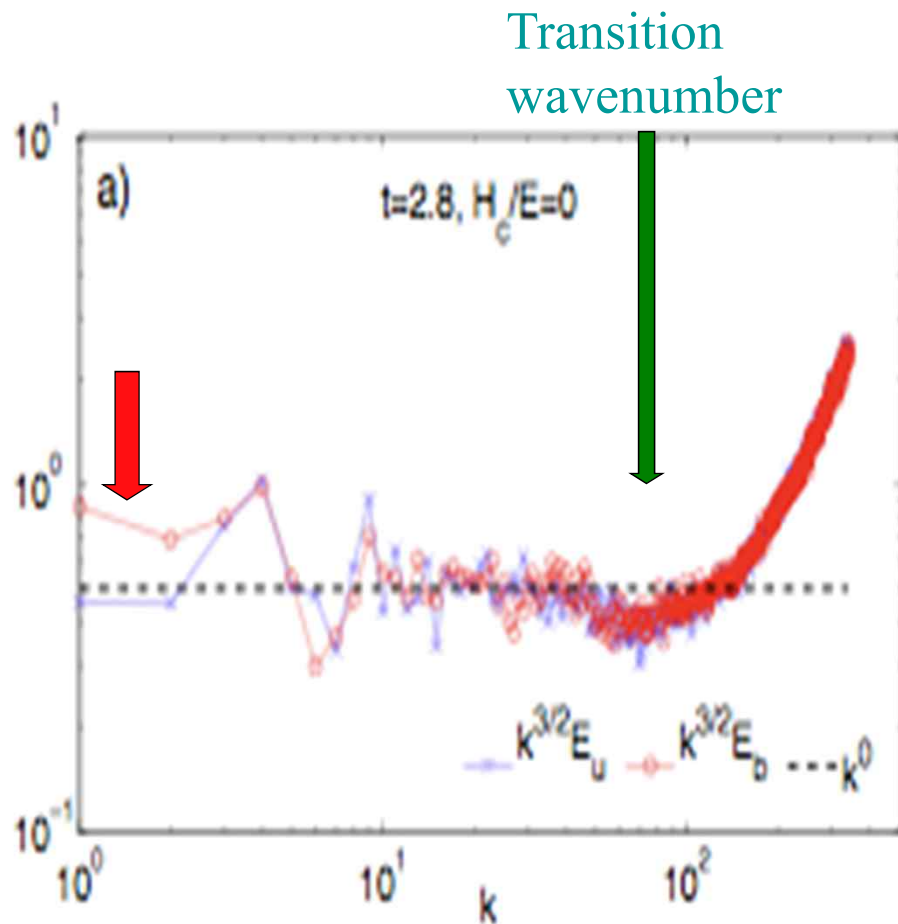
2D MHD: Krstulovic et al., PRE 2011



Ideal MHD in two dimensions ($\nu=0$ and $\eta=0$):

Kinetic & magnetic energy spectra, compensated by $k^{3/2}$

Intermediate temporal phase:
the small-scale thermalized k^{D-1} spectra act as eddy diffusivities for the “turbulent” dynamics at intermediate scales

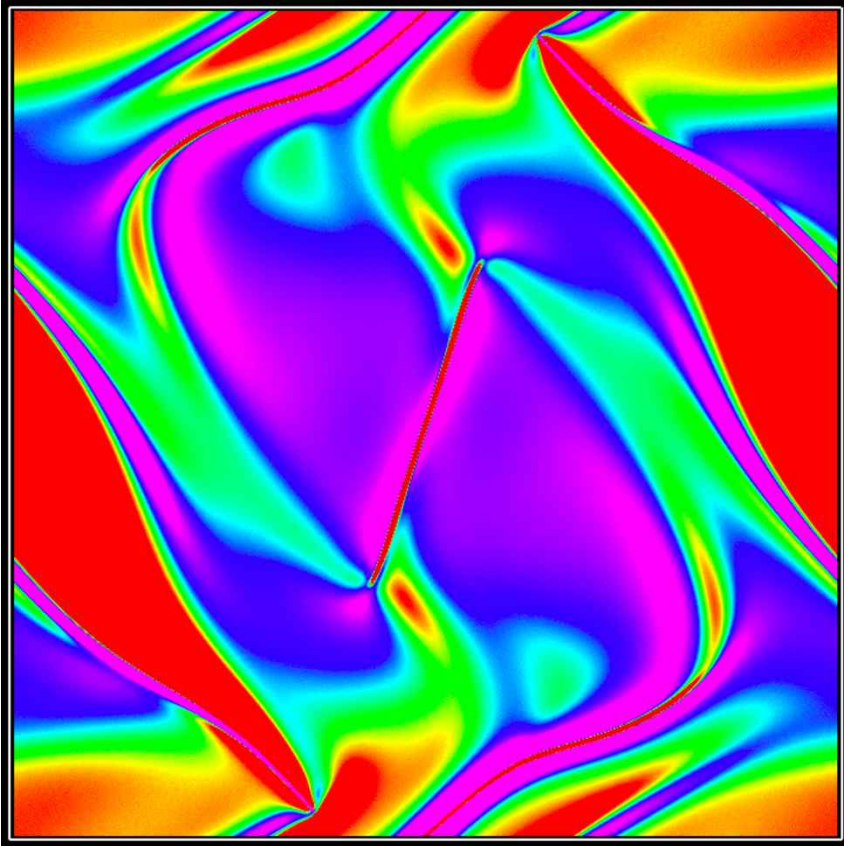


Ideal MHD in two dimensions ($\nu=0$ and $\eta=0$):

Kinetic & magnetic energy spectra, compensated by $k^{3/2}$

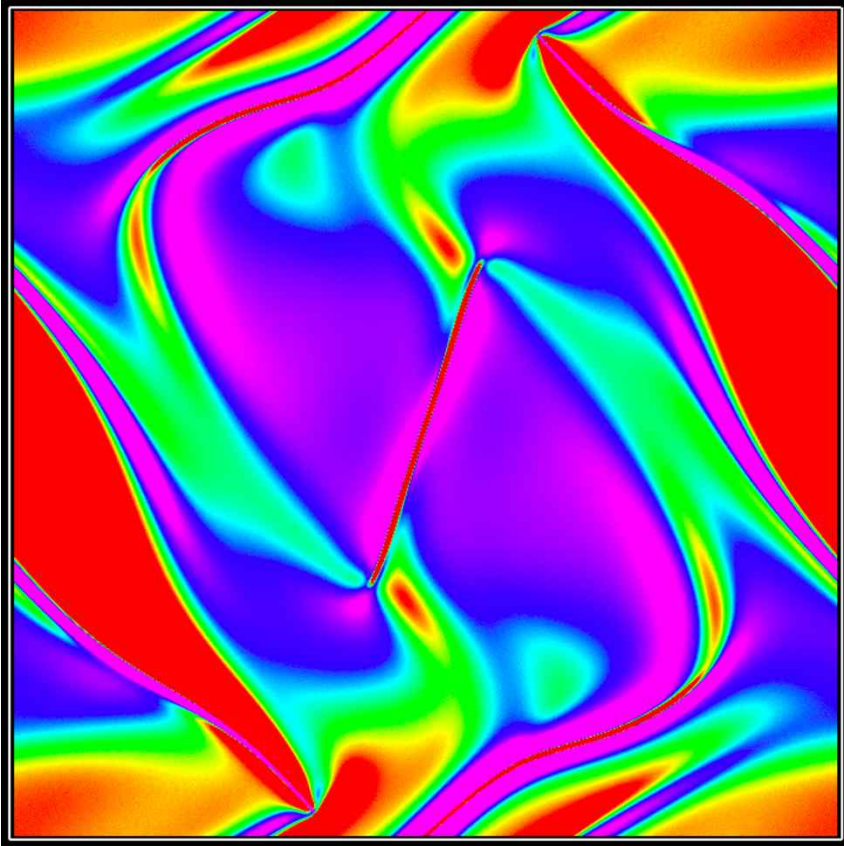
Intermediate temporal phase:
the small-scale thermalized k^{D-1} spectra act as eddy diffusivities for the “turbulent” dynamics at intermediate scales

Current sheets

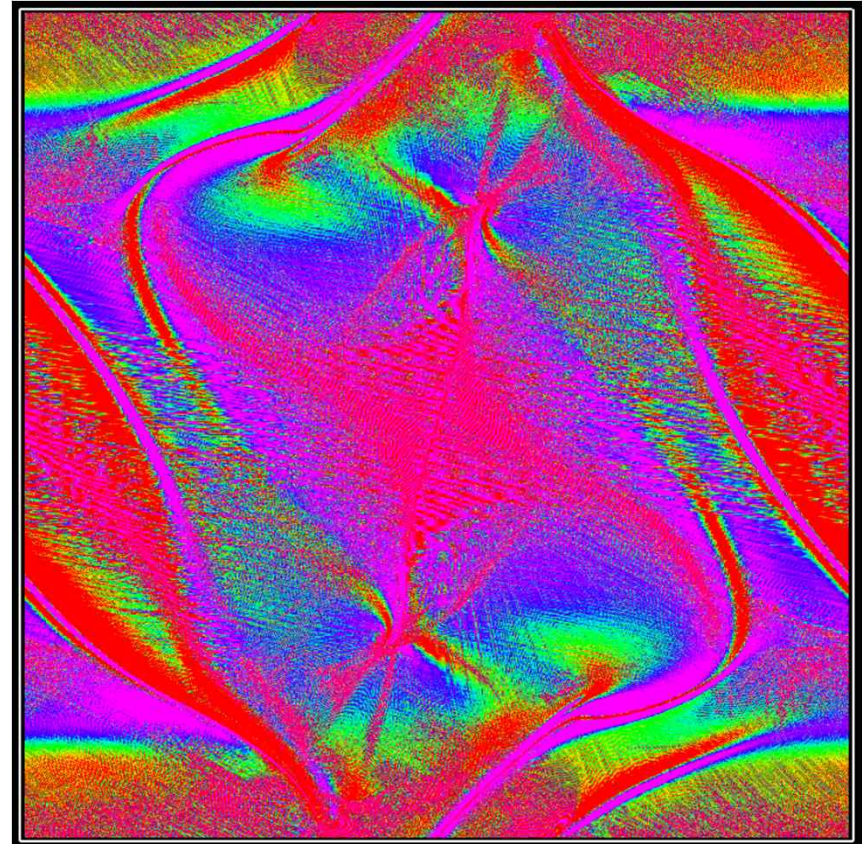


End of resolved phase

Current sheets

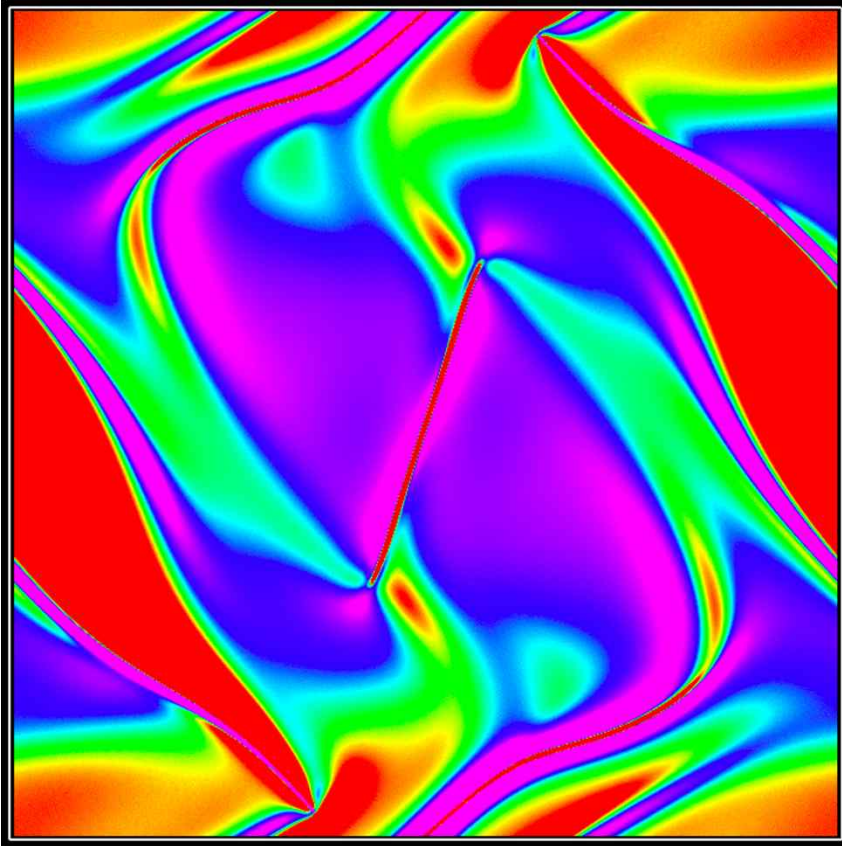


End of resolved phase

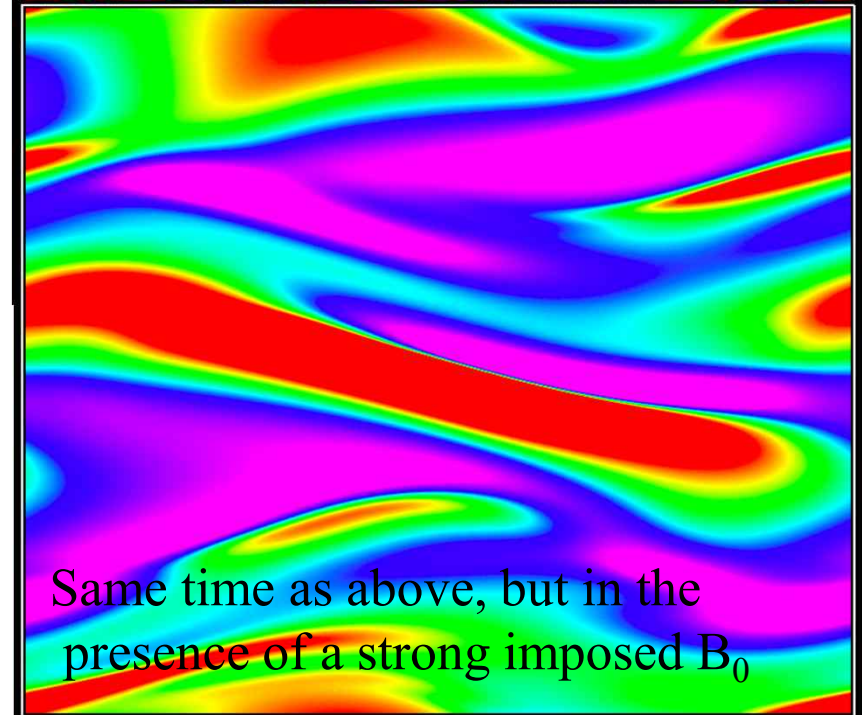
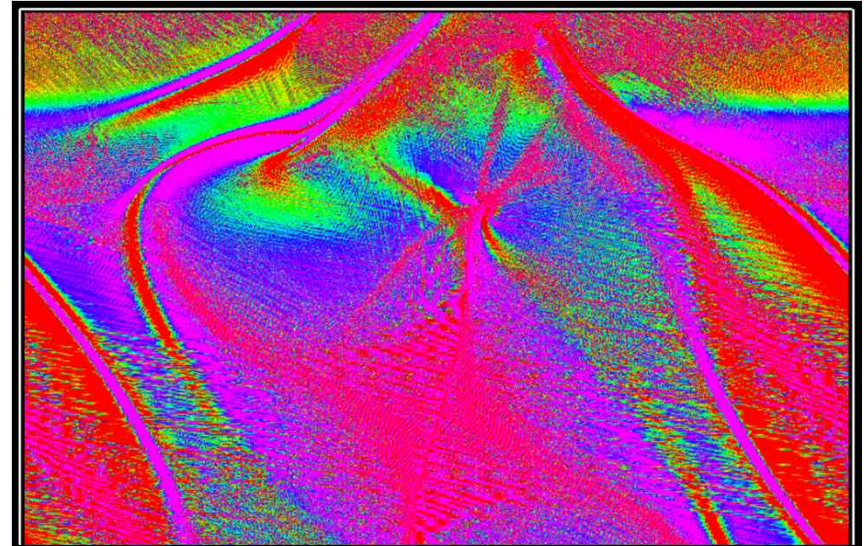


Later on, noise super-imposed
to current structures

Current sheets



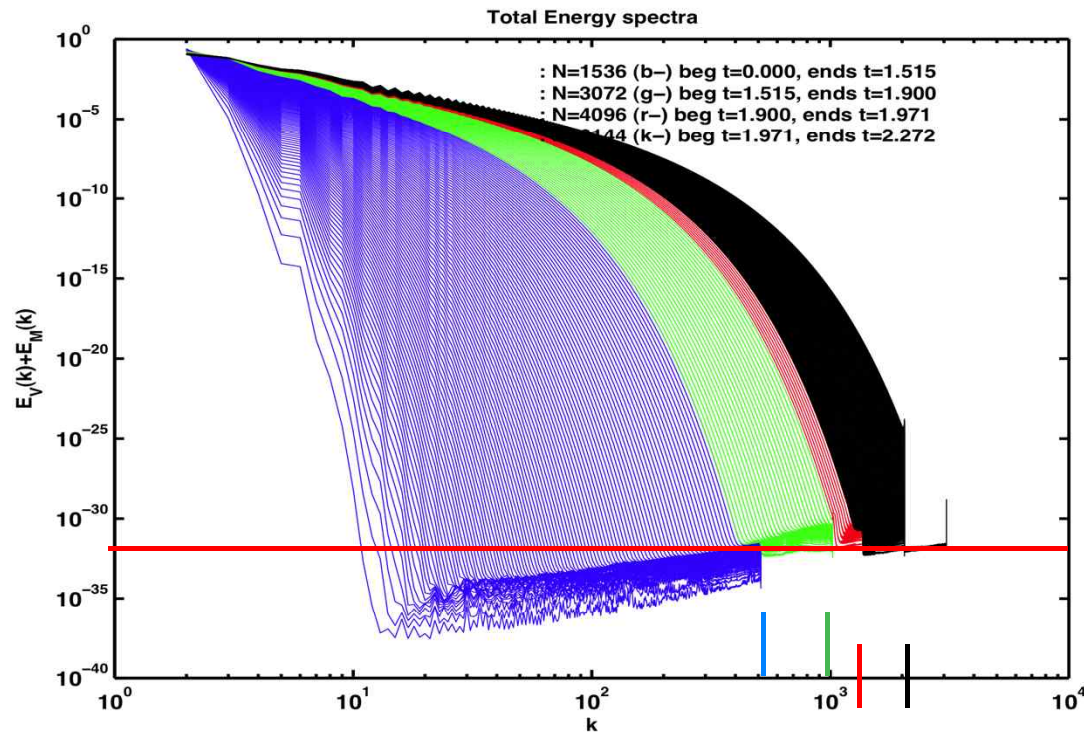
End of resolved phase



Same time as above, but in the presence of a strong imposed B_0

3D ideal dynamics in MHD, $B_0 = 0$

Total energy spectra, at
different times and
computed in a sequence of
runs at different
(*equivalent*) resolutions:



1536³

3072

4096

6144³

But is it reliable?

*INCITE (DOE) award
Rosenberg et al., in preparation*

3D ideal dynamics in MHD, $B_0 = 0$

Total energy spectra, at different times and computed in a sequence of runs at different (*equivalent*) resolutions:

1536³

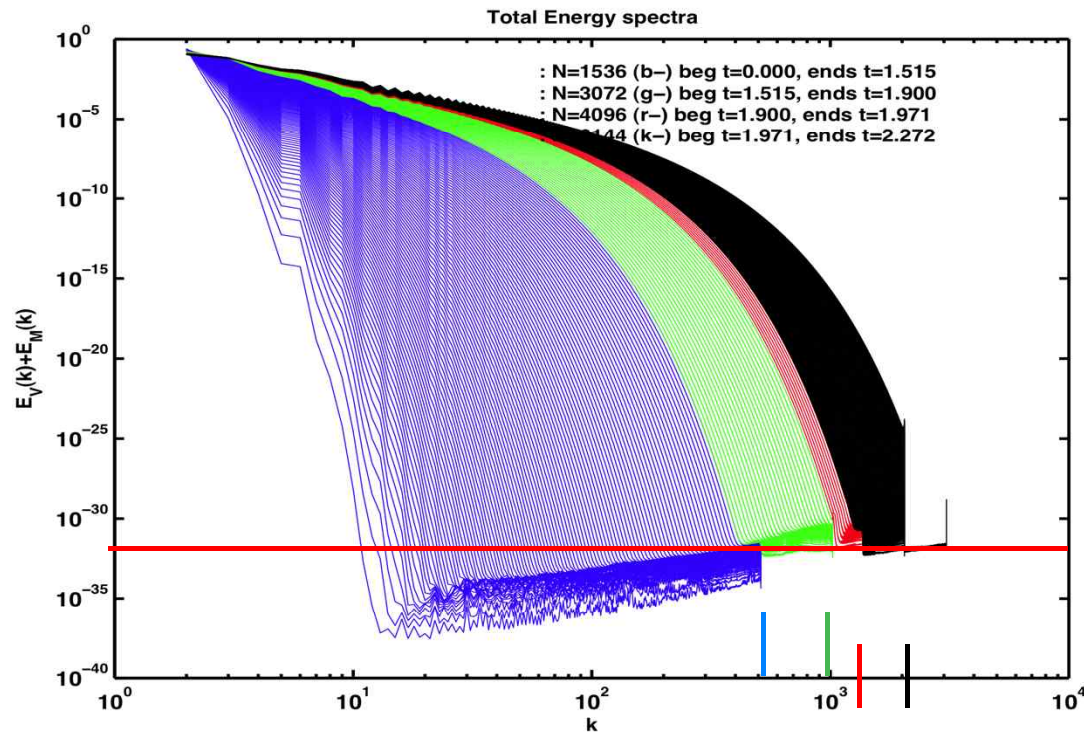
3072

4096

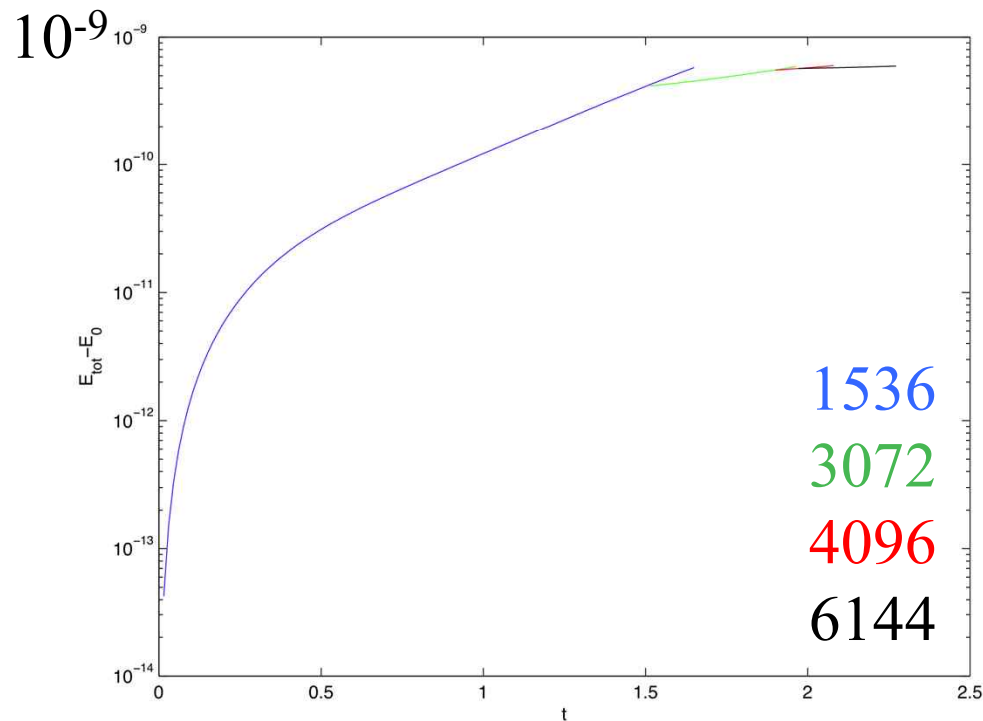
6144³

But is it reliable?

Anisotropy spectra with moderate B_0 : Grappin Mueller *PRE* 2010



INCITE (DOE) award



Ideal MHD in 3D

Temporal evolution of the total energy error ($E_T(0) \sim 1$):

$$E_T(\mathbf{t}) - E_T(\mathbf{0})$$

on grids with different resolutions
(with some temporal overlap)

In the future:

- Examine the ideal dynamics at high resolution (6144^3) for its singularity properties, up until the energy reaches the grid (log. decrement $\delta \sim \Delta x$)
- Continue the 4096^3 runs to long times to see the intermediate time & intermediate scale turbulent ideal dynamics with different initial conditions

Link with (fast) reconnection for the large-scale flow?

Third case study:

Small amounts of relative kinetic helicity can drive large-scale dynamos, given sufficient scale separation between the forcing scale & the largest resolved scale

Numerical set-up for Case 3

- Periodic boundary conditions, pseudo-spectral code, de-aliased with the 2/3 rule, *no imposed symmetries*
- Direct numerical simulations, from 192^3 to 512^3 points
- No imposed uniform magnetic field ($B_0=0$), $P_M=4$
- Velocity forcing at $1 < k_F / k_{\min} < 6$, $T_{\text{corr}} \sim 0.1$, $T_{\text{NL}} \sim 4.2$

Relative helicity f_h of the forcing between 1% and 90%

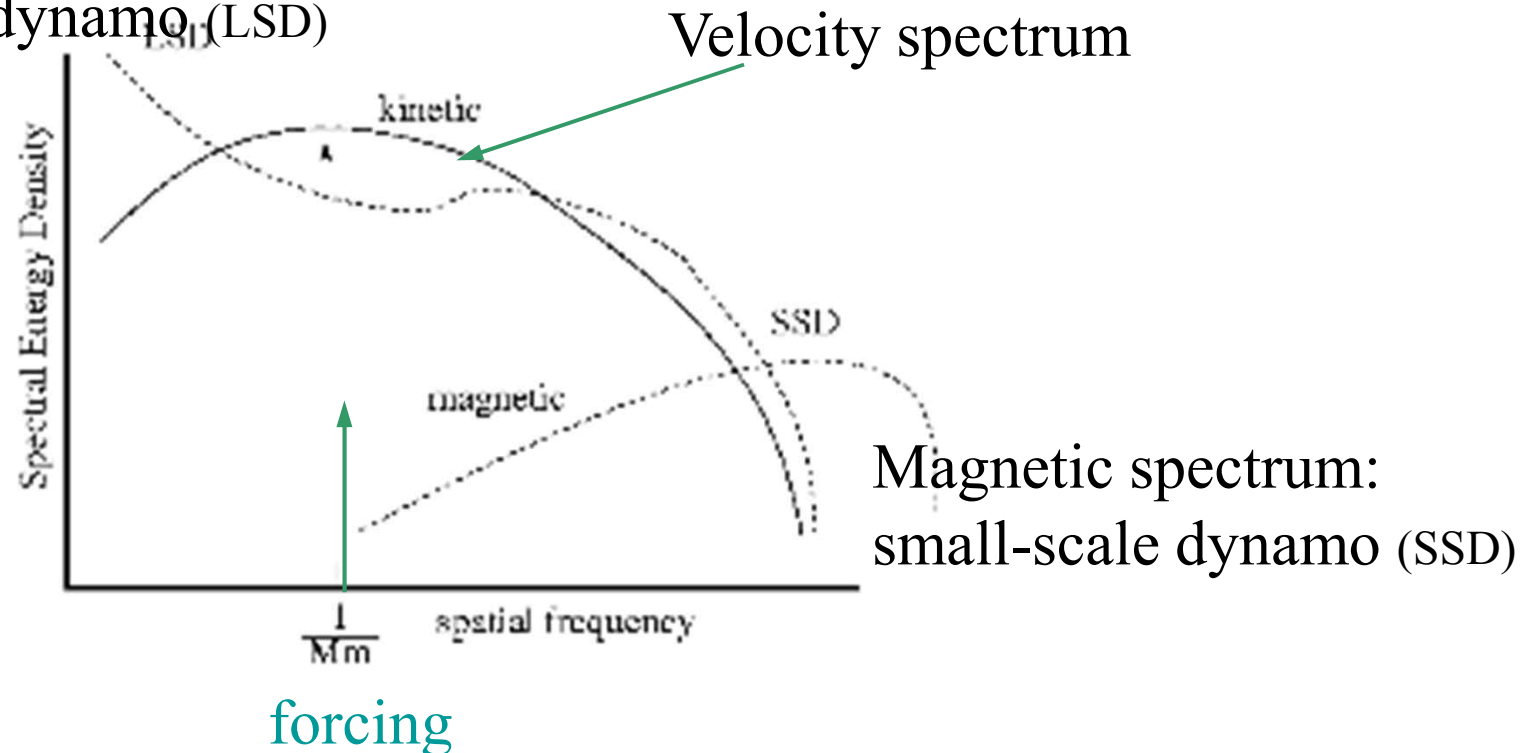
$$f_h = \langle u \cdot \omega \rangle / [\langle u^2 \rangle \langle \omega^2 \rangle]^{1/2}$$

GHOST

- **Geophysical High Order Suite for Turbulence** *(Gomez & Mininni)*
- **Community code**
- Pseudo spectral, incompressible Navier-Stokes (including rotation and passive scalar), and magnetic fields (MHD, with or w/o Hall term); it also includes some LES (the alpha model; a helical spectral model)
- The code parallelizes linearly up to 40,000 processors using hybrid Open-MP/MPI *(Mininni et al. 2011, Parallel Computing 37)*
- **Community Data** *(2048³ forced Navier-Stokes turbulence with and without helicity; 1536³ and 3072³ helically forced rotating turbulence; 1536³ decaying turbulence with a magnetic field, 2048³ MHD with symmetries). [3D visualization with VAPOR freeware]*

Small-scale (SSD) vs. Large-Scale (LSD) Dynamos

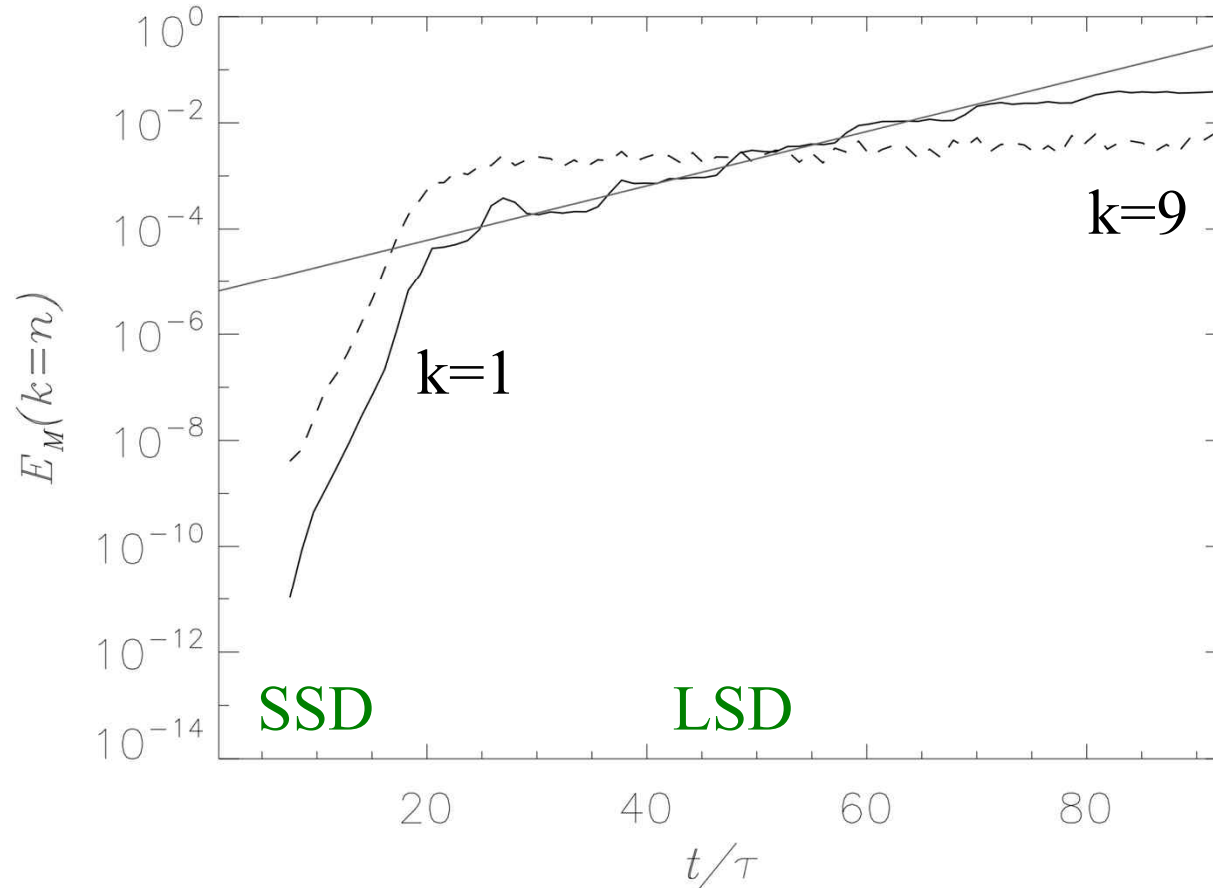
Magnetic spectrum:
large-scale dynamo (LSD)



Modal magnetic energy as a function of time

Run 384-60

$k_f=4$

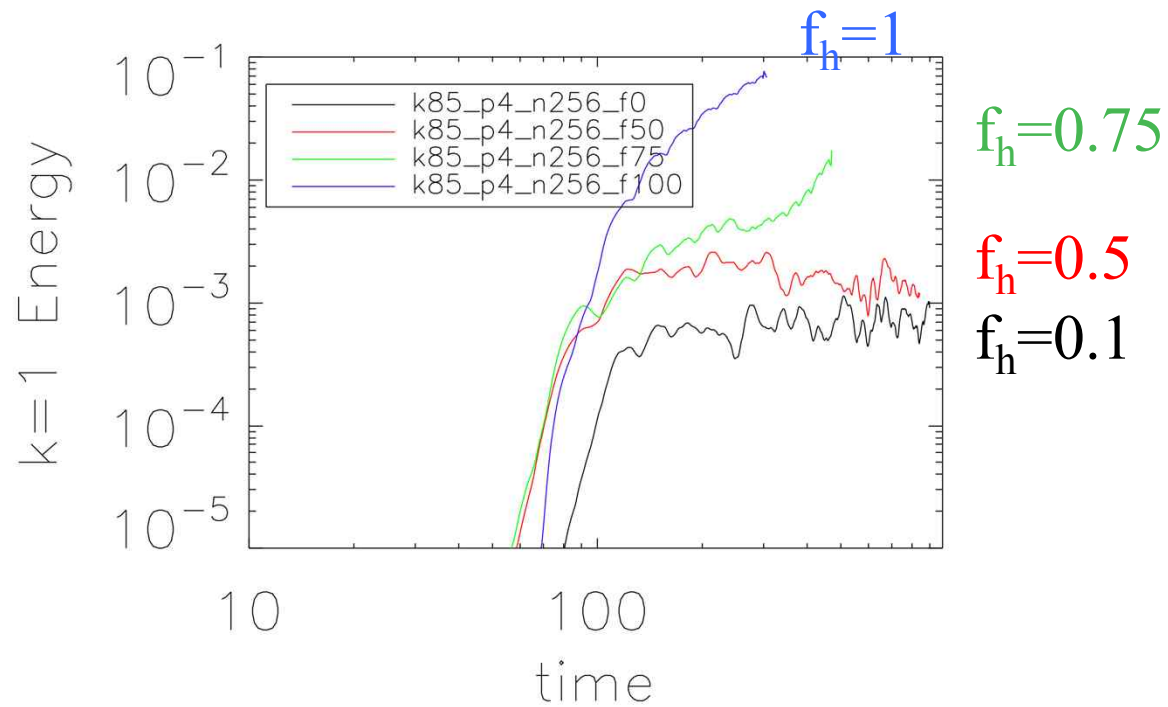


Saturation at small scale, continued slower growth at large scale

Conceptual framework

- Periodic dynamo, large-scale (LS) and small-scale (ss) fields;
relative helicity $H_R(\mathbf{k}) = H_V(\mathbf{k}) - k^2 H_M(\mathbf{k}) = H_V(\mathbf{k}) - H_J(\mathbf{k})$ (*PFL '76*)
- Small-scale field grows through stretching of field lines, like vorticity
- Large-scale field grows through relative helicity
- Early times: kinetic helicity responsible for growth of LS helical field
- Magnetic helicity conservation implies that large-scale M-helicity leads to small-scale M-helicity of the opposite sign
- The growth of B at large scale is responsible for the decrease of small-scale H_R (*through Alfvén waves: the faster the smaller the scale*), thereby stabilizing the LS field at some given scale

Growth of large-scale field ($k=1$) for different relative helicity



$N=256, k_f=3$

Kinetic and magnetic energy spectra as a function of k/k_f for **fixed 60% relative helicity**, after $90 T_{NL}$ and with two different scale separations

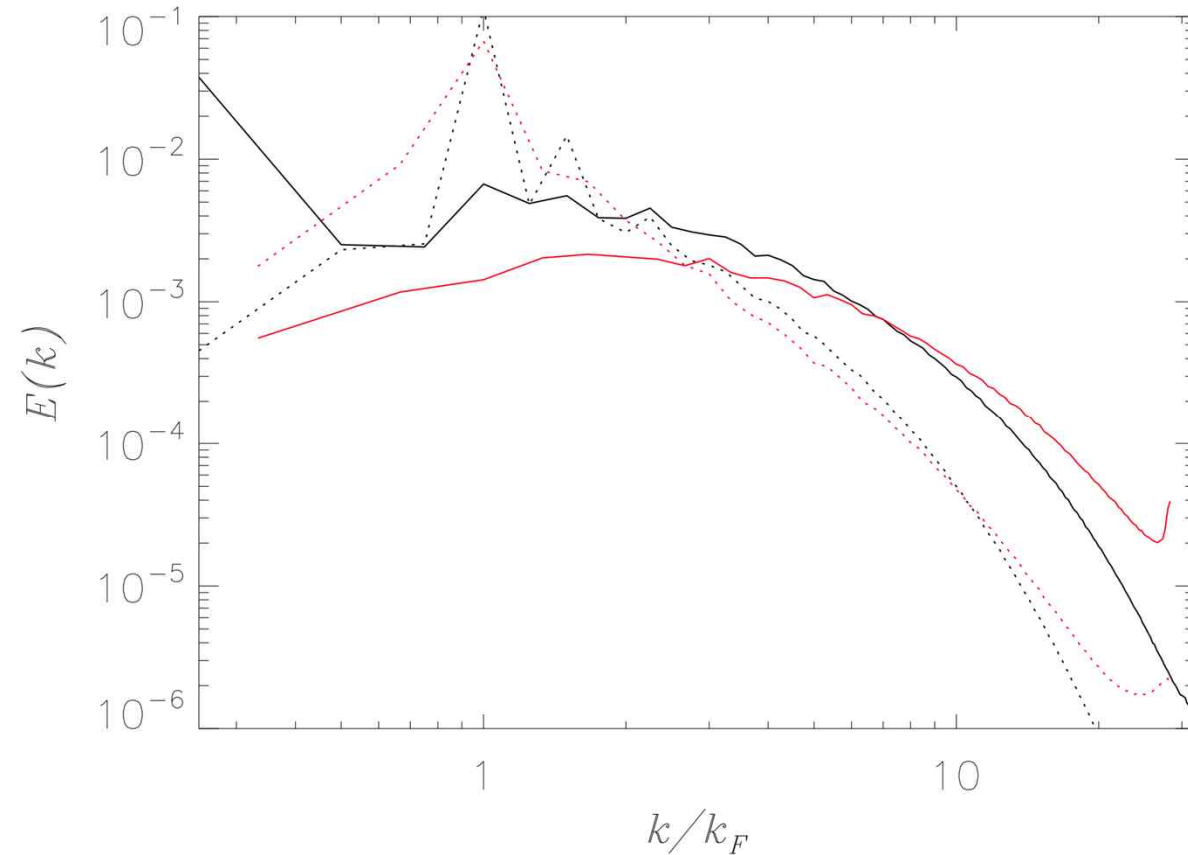
$384^3, k_f=4$

versus

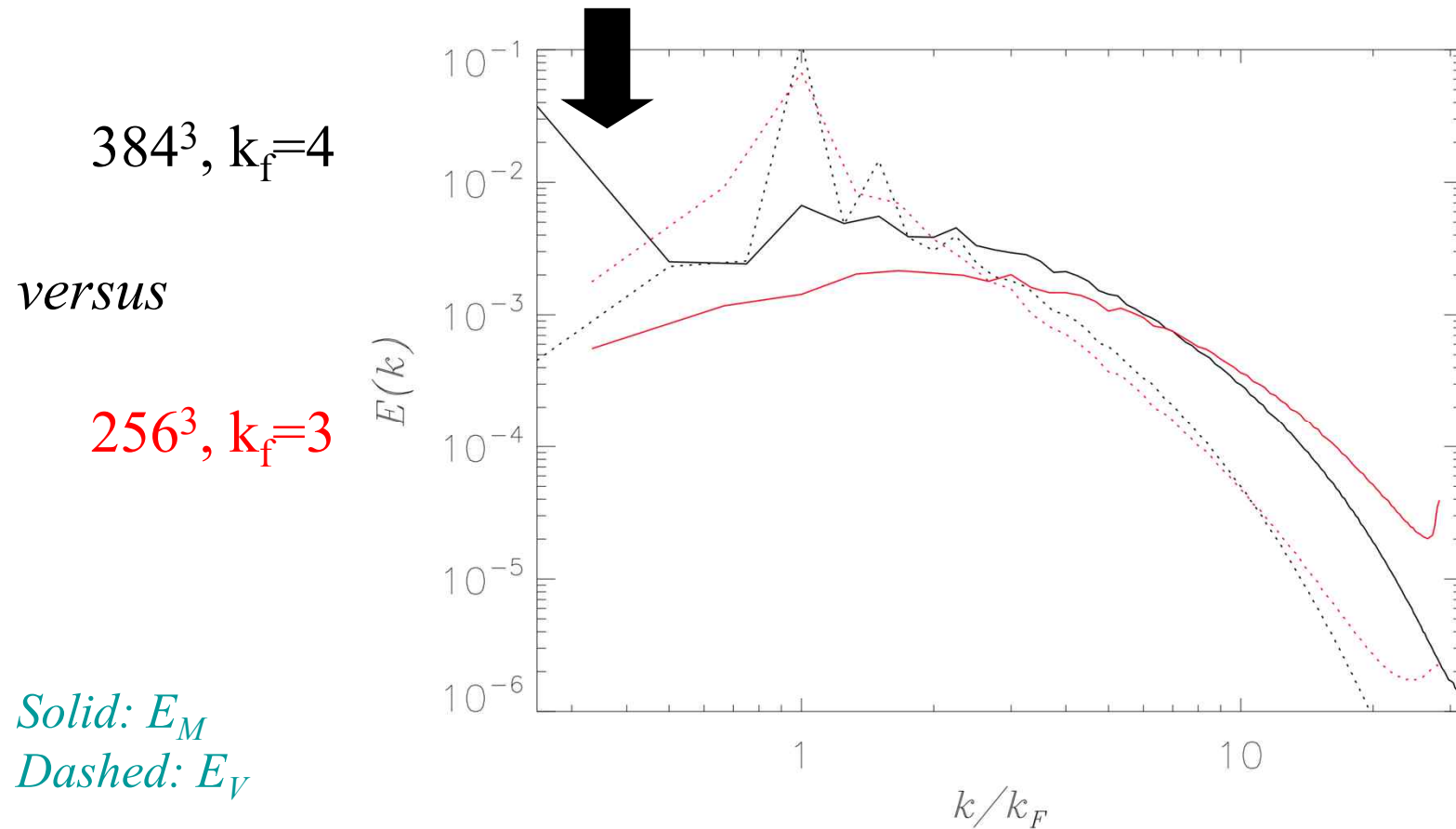
$256^3, k_f=3$

Solid: E_M

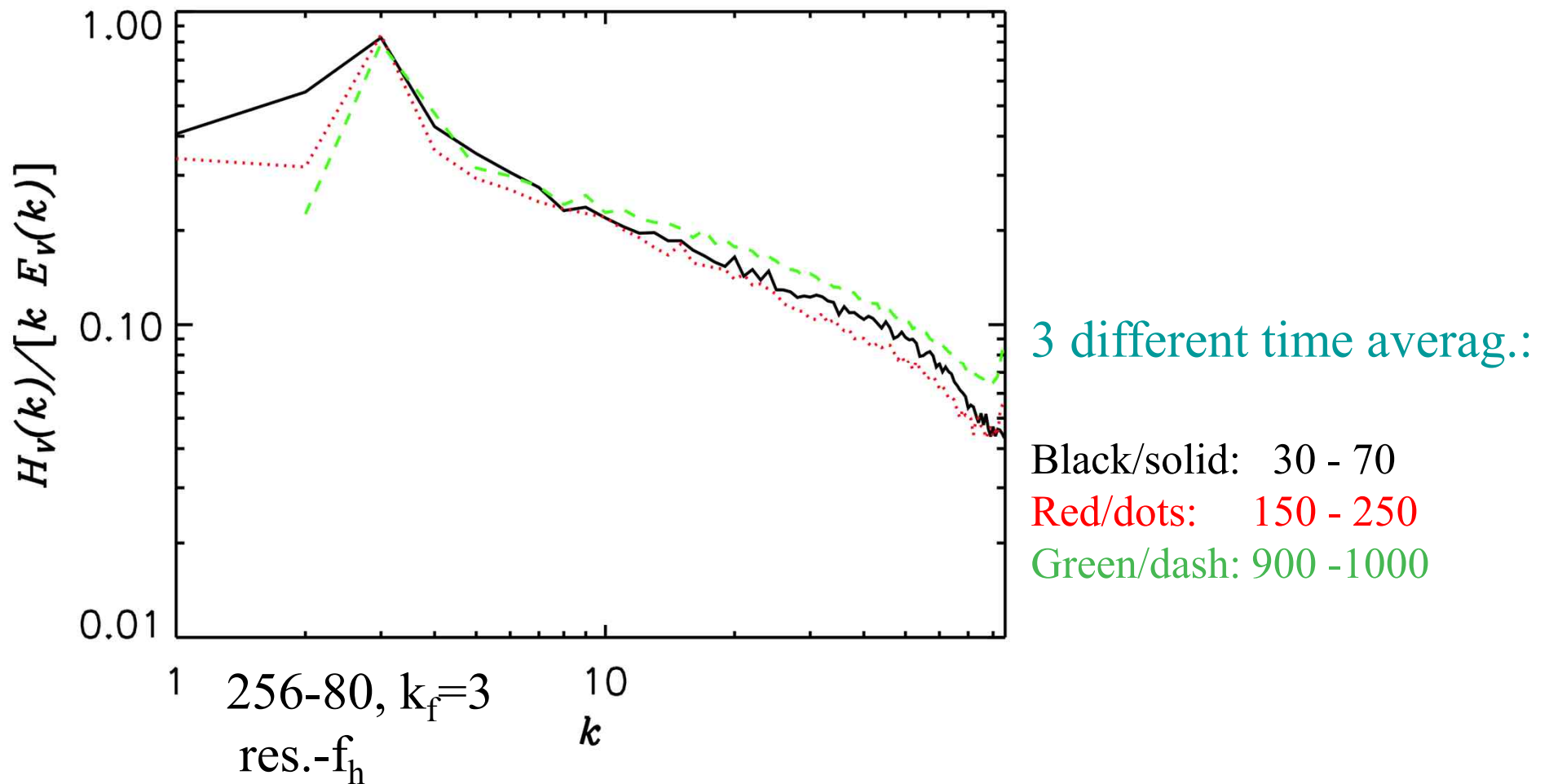
Dashed: E_V



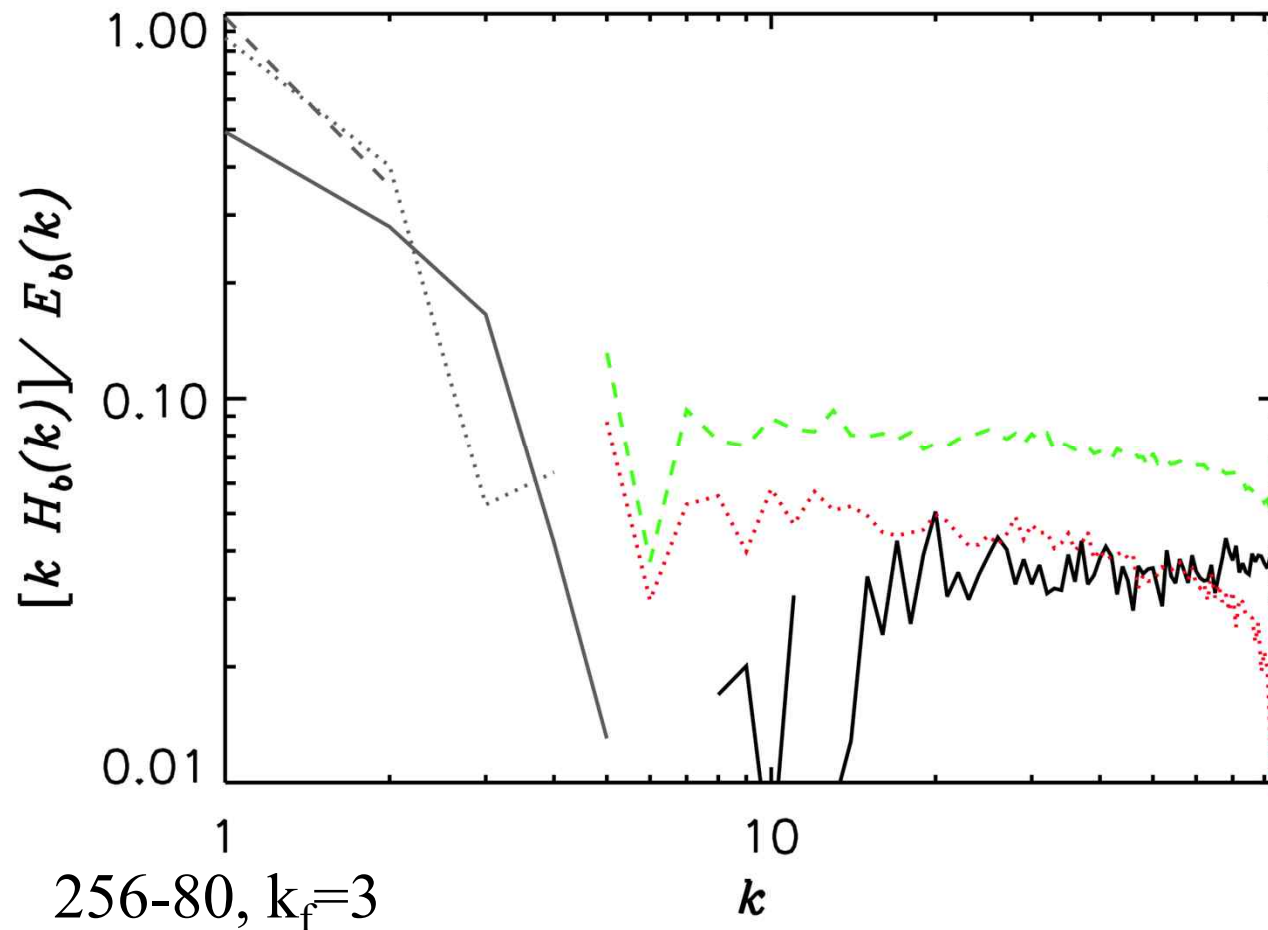
Kinetic and magnetic energy spectra as a function of k/k_f for **fixed 60% relative helicity**, after $90 T_{NL}$ and with two different scale separations



Spectra of the relative degree of alignment between the velocity field and the vorticity



Spectra of the relative degree of alignment of the magnetic field and magnetic potential

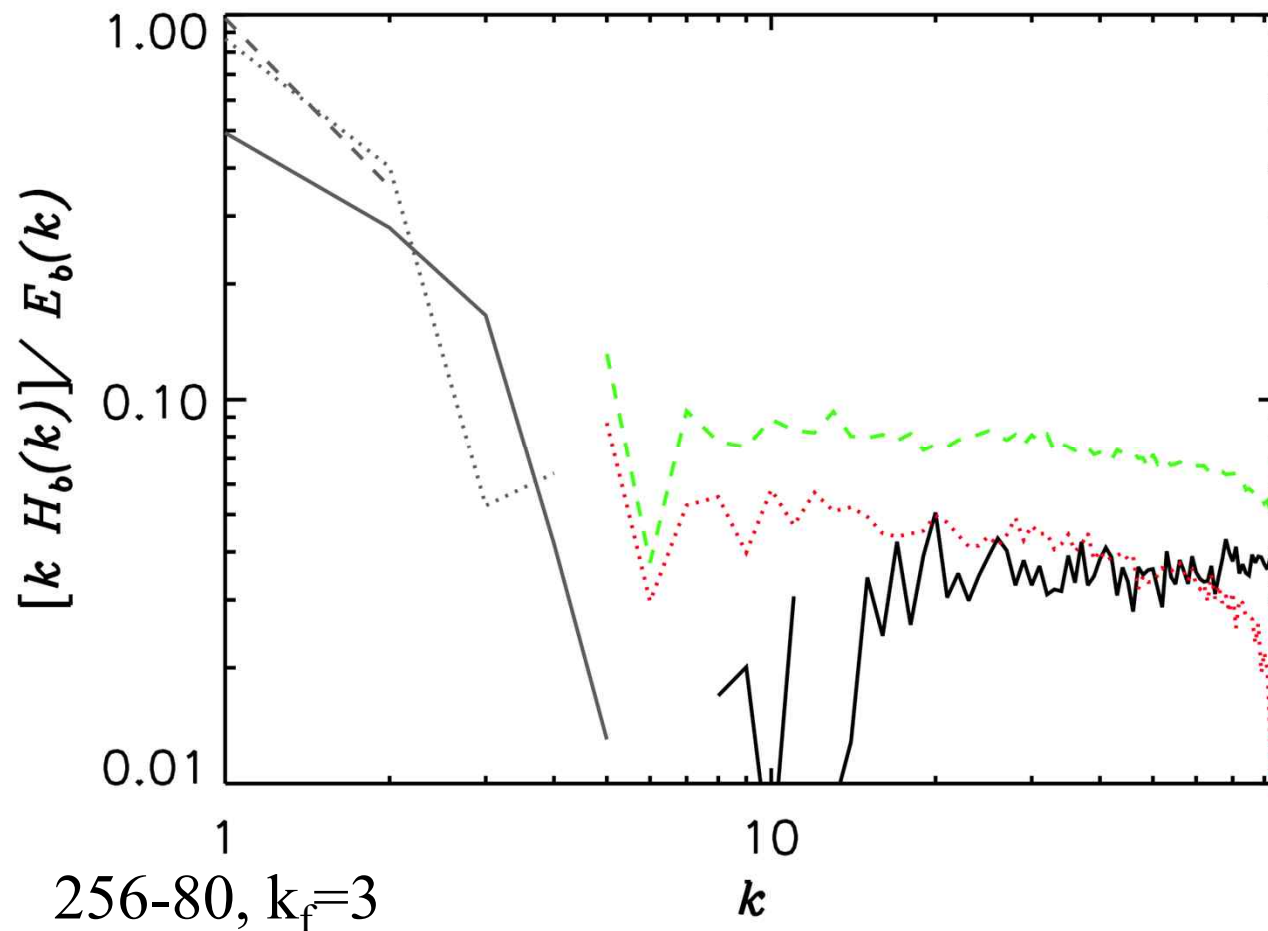


3 different times

$t_1 < t_2 < t_3$

solid dot dash

Spectra of the relative degree of alignment of the magnetic field and magnetic potential



Large-scale
force-free
field

3 different times

$t_1 < t_2 < t_3$

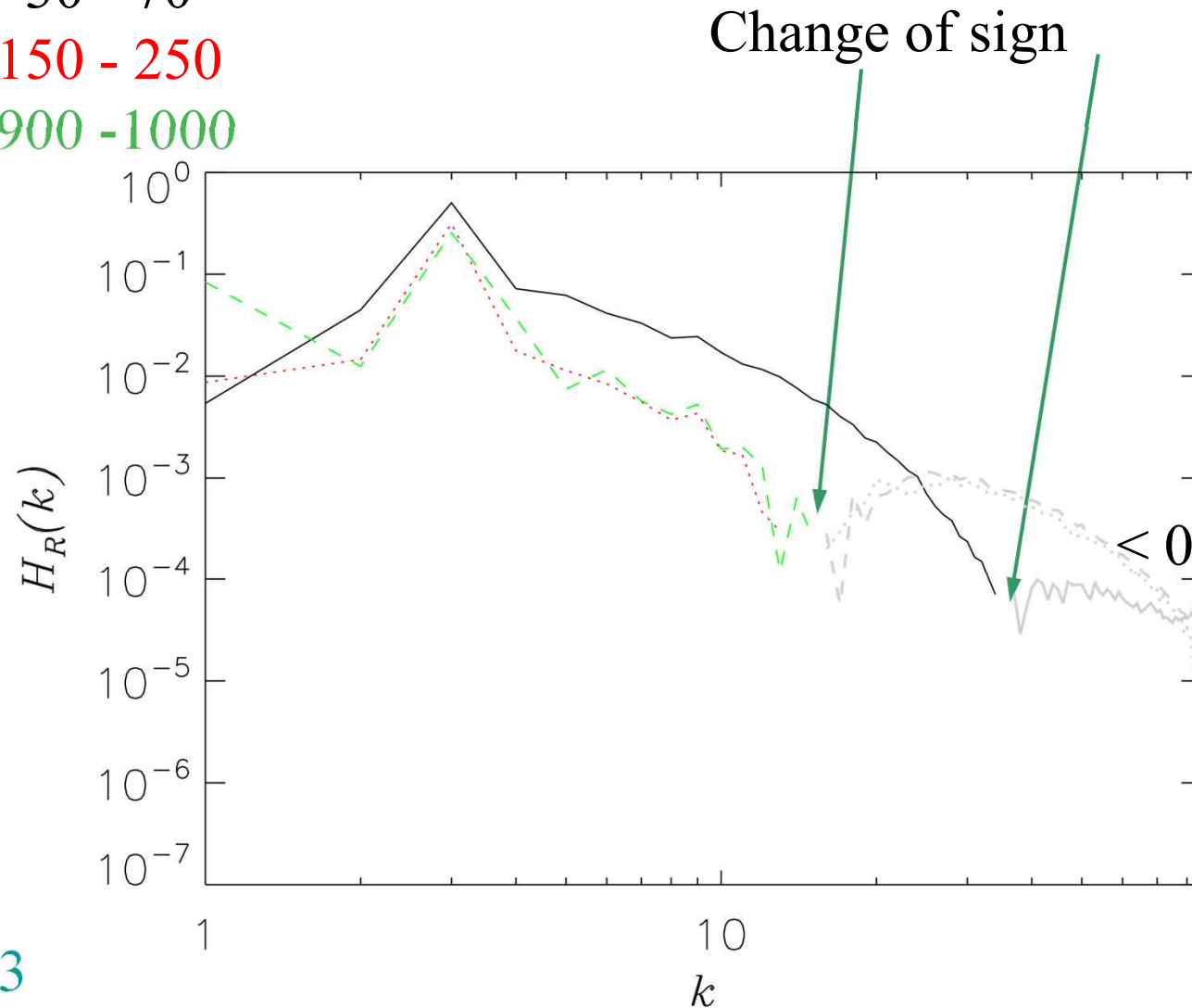
solid dot dash

Residual helicity $H_R(K)=H_V-k^2H_M$
Temporal average in [., .]

Black/solid: 30 - 70

Red/dots: 150 - 250

Green/dash: 900 -1000



256-80, $k_f=3$

Previous numerical study of that issue:

Maron & Blackman 2002

- $f_h \equiv \langle \mathbf{v} \cdot \boldsymbol{\omega} \rangle / \sqrt{\langle v^2 \rangle \langle \omega^2 \rangle}$
- 64^3 simulation
- Forcing wavenumber,
→ $k_F = 4.5$
- $Re_M \sim 150$
- Critical threshold
 - • $f_{h,C} \sim 0.5$ for
 $Pr_M = 3$
 - • $f_{h,C} \sim 0.7$ for
 $Pr_M = 9$

→ One needs a substantial amount of relative helicity for such parameters

Runs with resolutions from 192^3 to 512^3 , with forcing at $k_F=1$ to 6, with relative helicity of the forcing between 1% and 90%, $T_{NL} \sim 4$, and with magnetic Reynolds number Re_M of the order of 2000

k_F	Run	Re_M	k_{seed}	γ_{SSD}	$\gamma_{k=1}$	E_b^s	$-100H_b$
2	192-70	1500	[6.7,10.7]	0.26	$(-5.6 \pm 2.8)10^{-3}$	0.2	0.85f
	192-80	1600	–	0.25	$(-8.2 \pm 2.8)10^{-3}$	0.25	0.85f
	192-90	1600	–	0.27	$(4.8 \pm 12)10^{-3}$	0.25	1.5g
3	256-40	1900	[10,16]	0.28	$(-0.7 \pm 7.8)10^{-4}$	0.1	0.1f
	256-60	1900	–	0.29	$(1.3 \pm 7.5)10^{-4}$	0.1	0.2f
	256-69	1700	–	0.26	$(5.9 \pm 0.7)10^{-3}$	0.1	1.0g
	256-80	1900	–	0.31	$(8.3 \pm 1.5)10^{-3}$	0.15*	3g*
4	384-10	1600	[13.3,21.3]	0.24	$(-1.6 \pm 2.0)10^{-3}$	0.04	0.008f
	384-20	1600	–	0.29	$(5.9 \pm 0.6)10^{-3}$	0.04	0.06g

Res- f_h

Small-scale growth rate

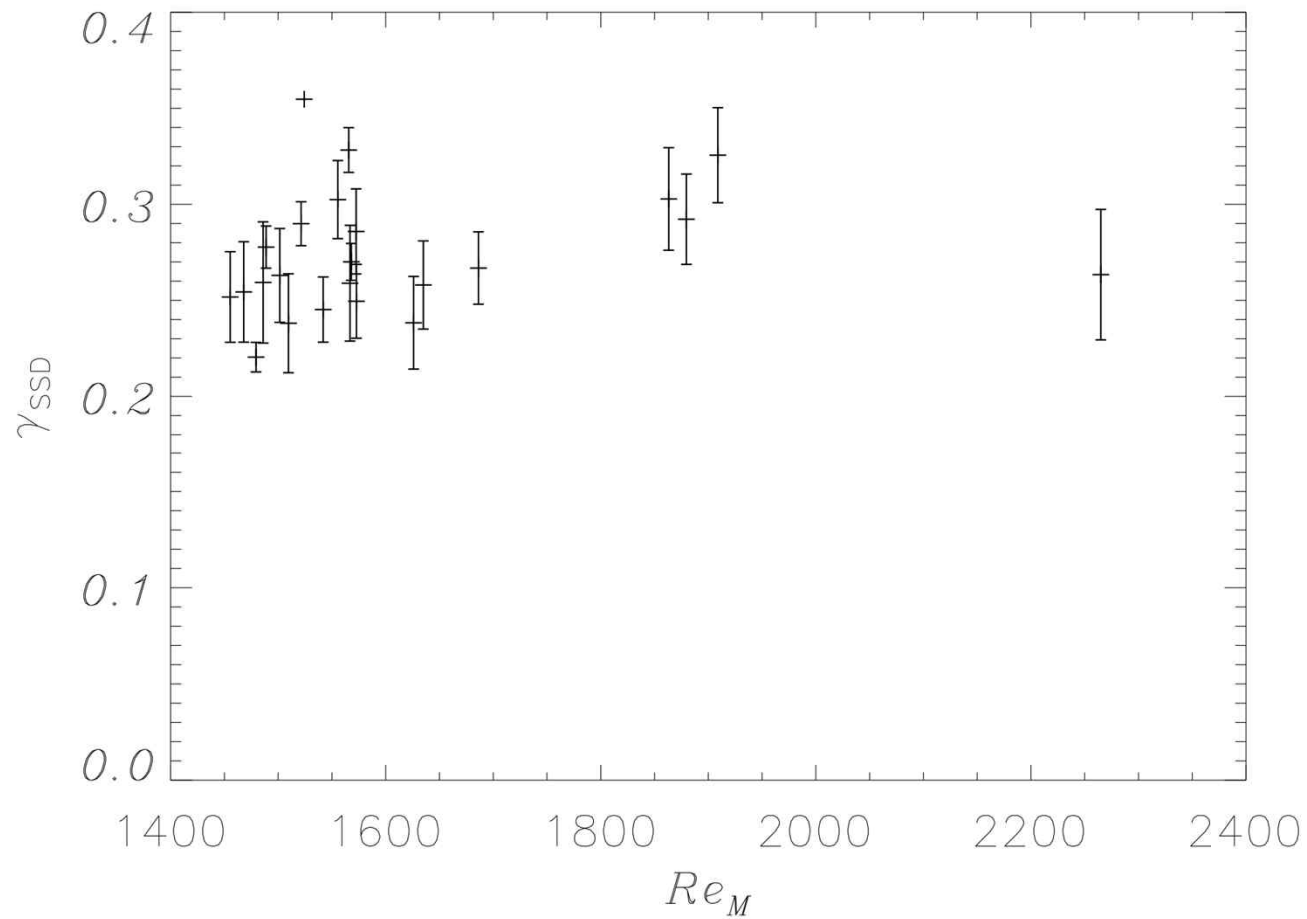
Large-scale growth rate after saturation of the SSD

Run	Re_M	k_{seed}	γ_{SSD}	$\gamma_{k=1}$	E_v^2	$-100H_b$	k_F
384-40	1500	[13.3,21.3]	0.24	$(1.5 \pm 0.1)10^{-2}$	N/A	N/A	
384-60	1500	–	0.25	$(2.8 \pm 0.2)10^{-2}$	0.1	1.0g	4
384-80	1500	–	0.27	$(2.8 \pm 0.3)10^{-2}$	N/A	N/A	
432-05	2100	[16.7,26.7]	0.24	$(-1.2 \pm 2.9)10^{-3}$	0.04	0.008f	
432-07	2000	–	0.23	$(0.6 \pm 3.9)10^{-3}$	0.03	0.004f	5
432-09	2000	–	0.24	$(1.1 \pm 0.4)10^{-2}$	0.03	0.004g	
512-01	1500	[20,32]	0.21	$(6.1 \pm 6.1)10^{-3}$	0.01	$\pm 5 \cdot 10^{-4}f$	
512-05	1500	–	0.21	$(3.3 \pm 0.7)10^{-2}$	0.01	$1.2 \cdot 10^{-3}g$	6

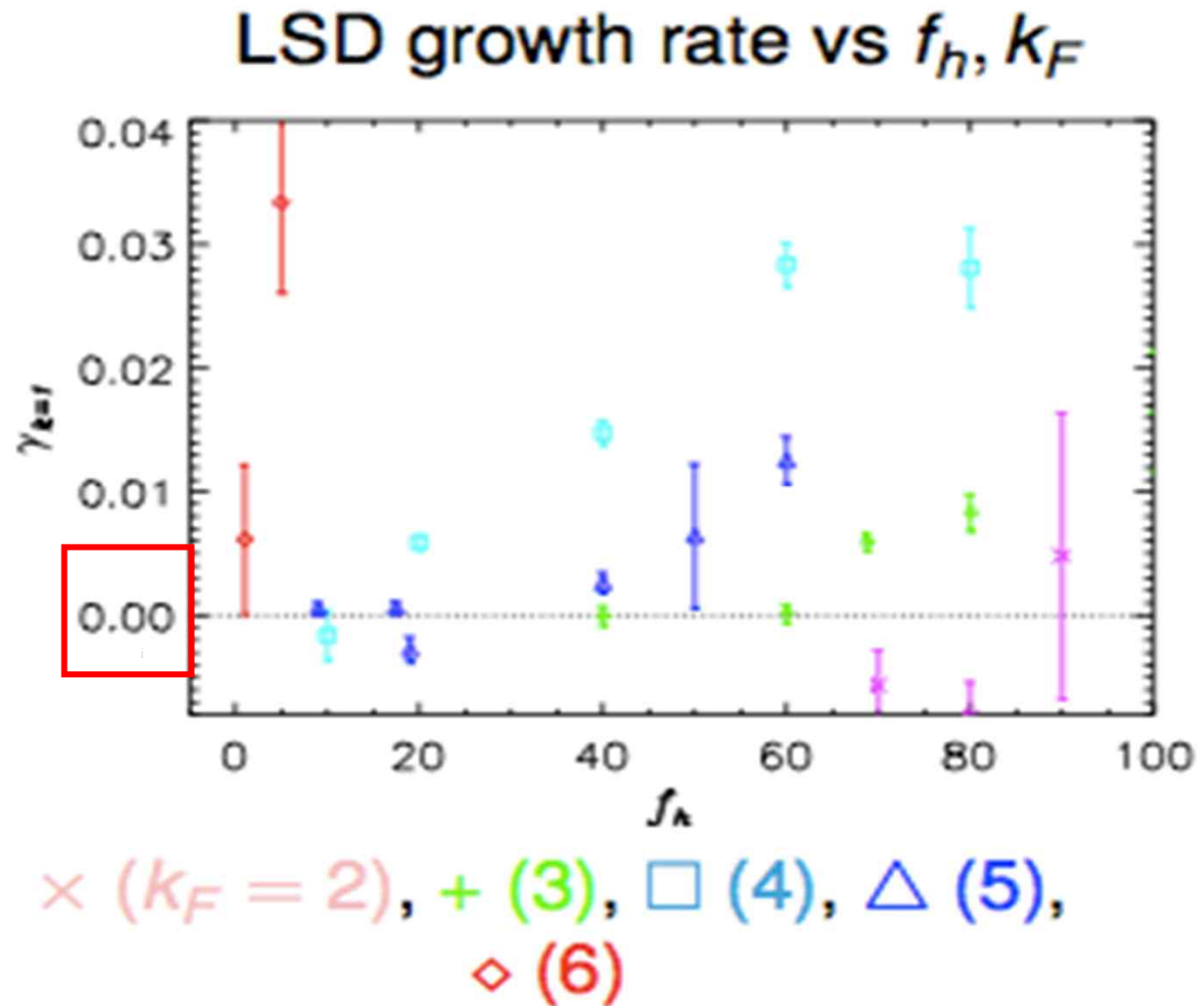
Res- f_h

Small-scale vs. Large-scale
growth rates

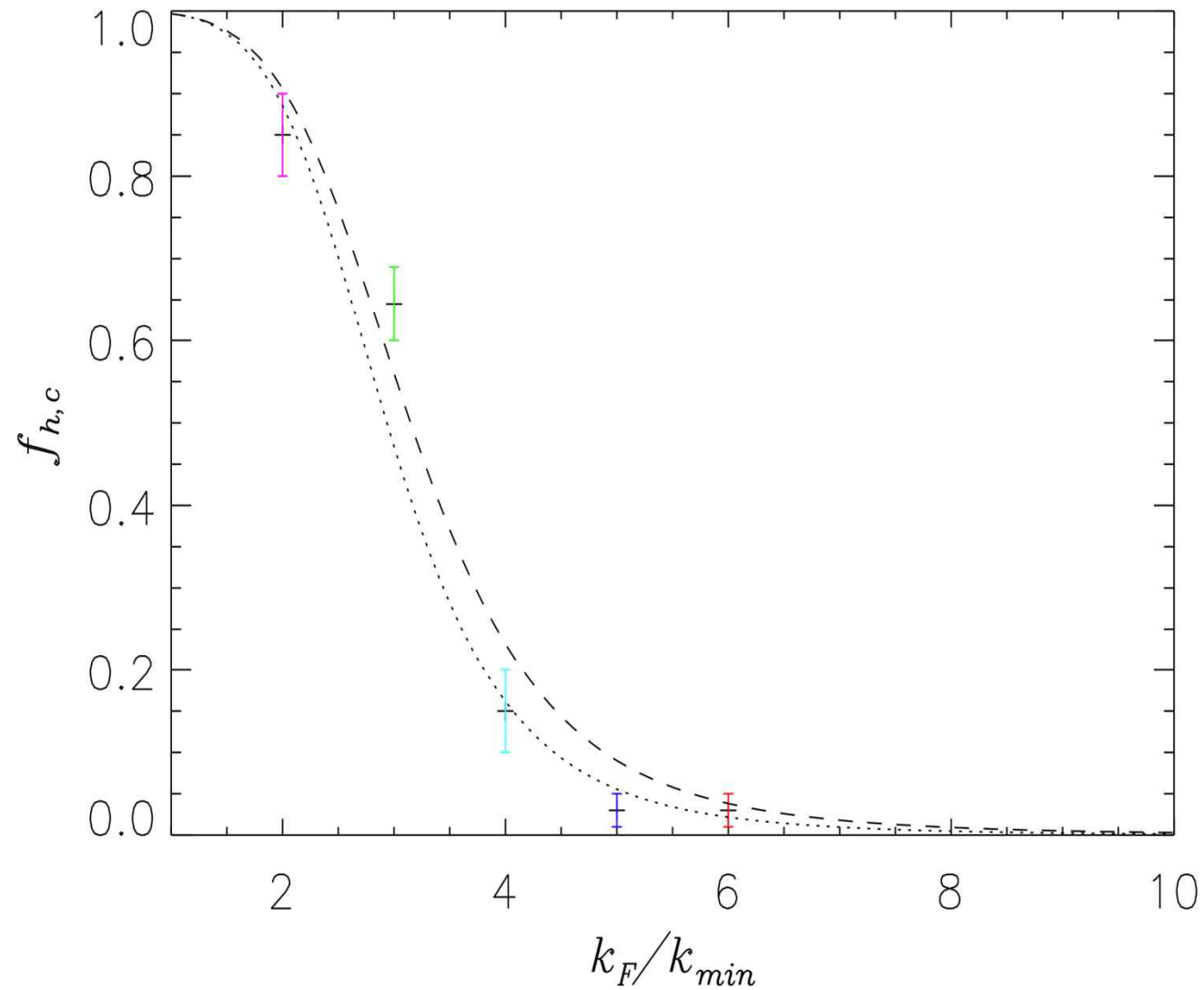
Growth rate of small-scale field as a function of magnetic Reynolds number



Large-scale growth-rate as a function of relative helicity f_h
for various scale separation (forcing wavenumber k_f)



Critical rate of helicity for large-scale dynamo as a function of forcing scale separation



Simple theory

- Near end of kinematic, linear SSD phase $\Rightarrow \sqrt{1 - f_h} B^2$
non-helically-produced, $\sqrt{f_h} B^2$ helically-produced
- Non-helically-produced $\mathbf{j} \times \mathbf{B}$ opposes LSD
- $\boldsymbol{\omega} \times \mathbf{v}$ generates LSD
- Kazantsev $B(k)^2 \sim k^{3/2}$ spectrum $\Rightarrow [\mathbf{j} \times \mathbf{B}](k_{min}) \sim (k_{min}/k_F)^{5/2}$
- $\sqrt{1 - f_h}(k_{min}/k_F)^{5/2} \propto \sqrt{f_h}$
- $f_{h,C} = (1 + C^2(k_F/k_{min})^{-5})$ where $C = (k_{min} v_{rms}^2)/(k_{SS} B_F^2)$
- $f_{h,C} \sim (k_F/k_{min})^{-5}$ as $k_F/k_{min} \rightarrow \infty$

Conclusion and questions

- With sufficient scale separation, at a given magnetic Reynolds number, the large-scale field grows, with $f_h^c < 0.05$ for $k_F=6$
- * *Does the result persist when one increases the Reynolds number?*
Park & Blackman, 2011
- * *What is the effect of the magnetic Prandtl number?*
- * *Is there an even/odd variation in growth rates & f_h^c ?*

Thank you for your attention!

